Range-Based Underwater Vehicle Localization in the Presence of Unknown Ocean Currents: Theory and Experiments

Mohammadreza Bayat, Naveena Crasta, António Pedro Aguiar, *Member, IEEE*, and António M. Pascoal, *Member, IEEE*

***Abstract*— This paper addresses the problem of range-based autonomous underwater vehicle (AUV) localization in the presence of unknown ocean currents. In the setup adopted, the AUV is equipped with an attitude and heading reference system, a depth sensor, and an acoustic device that provides measurements of its distance to a set of stationary beacons. We consider the situation where the number of active beacons is not known in advance and may vary with time. The objective is to simultaneously localize the AUV and beacons, that is, to find their positions underwater. We start by deriving conditions under which it is possible to reconstruct the initial condition of the system under study. We consider the design model where the states evolve continuously with time, but the range measurements are only available at discrete instants of time, possibly in a nonuniform manner. For trimming maneuvers that correspond to AUV trajectories with constant linear and angular velocities expressed in the body frame, we show that if either the position of one of the beacons or the initial position of the AUV is known, then even without depth information the system is weakly observable (i.e., the set of states that are indistinguishable from a given initial configuration contains only a set of finite isolated points). If depth measurements are also available, then the system is observable even in the presence of unknown constant ocean currents. Equipped with these results, we then propose a novel observer for simultaneous AUV and beacon localization. The mathematical setup exploited borrows from minimum-energy estimation theory applied to continuous-time processes with discrete measurements, projection filters, and multiple-model estimation techniques. Convergence analysis of the resulting observer system yields conditions under which the estimation errors converge to a small neighborhood of the origin (whose size depends on the magnitude of the process and measurement noise). The results of field experiments with a robotic marine vehicle show the efficacy of the simultaneous AUV/multiple beacon localization system proposed.**

***Index Terms*— Autonomous underwater vehicles (AUVs), minimum-energy (ME) observers, observability analysis, range-based underwater localization.**

Manuscript received June 29, 2014; revised December 9, 2014; accepted March 6, 2015. Manuscript received in final form March 27, 2015. This work was supported in part by the European Commission through the CADDY Project (FP7-ICT-2013) under Grant 611373 and in part by the Foundation for Science and Technology under Grant UID/EEA/50009/2013. The work of M. Bayat was supported by a Ph.D. Scholarship from the Foundation for Science and Technology, Portugal. Recommended by Associate Editor A. Alessandri. *(Corresponding author: Mohammadreza Bayat.)*

M. Bayat and N. Crasta are with the Institute for Systems and Robotics, Instituto Superior Técnico, University of Lisbon, Lisbon 1049-001, Portugal (e-mail: mbayat@isr.ist.utl.pt; ncrasta@isr.ist.utl.pt).

A. P. Aguiar is with the Research Center for Systems and Technologies, Faculty of Engineering, University of Porto, Porto 4200-465, Portugal (e-mail: pedro.aguiar@fe.up.pt).

A. M. Pascoal is with the Institute for Systems and Robotics, Instituto Superior Técnico, University of Lisbon, Lisbon 1049-001, Portugal, and also with the National Institute of Oceanography, Goa 403-004, India (e-mail: antonio@isr.ist.utl.pt).

Color versions of one or more of the figures in this paper are available online at http://ieeexplore.ieee.org.

Digital Object Identifier 10.1109/TCST.2015.2420636

I. Introduction

AUTONOMOUS underwater vehicles (AUVs) are steadily becoming the tool of choice for the execution of a vast number of scientific and commercial missions at sea that include ocean data acquisition, remote sensing, and mapping of the spatial extent of pollutant spills, to name a few. Meeting these objectives requires that the AUVs be equipped with cost effective and easy to install and use underwater navigation systems. Meeting this challenge may prove formidable, in view of the fact that conventional methods of vehicle localization that rely on GPS techniques cannot be used underwater, due to the high attenuation of electromagnetic signals.

The above problem can in principle be overcome by resorting to high-performance inertial navigation systems (INS). However, the cost of such systems may be prohibitive. Moreover, even with such high-performance INS, drift is inevitable. Other possible solutions involve the use of acoustic-based systems that rely on the measurements of the ranges between an AUV and a number of transponders in a baseline configuration or on the computation of range as well as bearing and elevation angles to a subsea transponder using an array of hydrophones that detect the incoming wave emitted by the transponder in response to a query by the AUV, see [1] for the description of localization techniques that include ultra short baseline (USBL), long baseline (LBL), and GPS intelligent buoy (GIB) systems. In practice, acoustic localization systems are often affected by the presence of outliers, latency, and multipath effects. In spite of this, however, acoustic-based methods for underwater vehicle navigation are pervasive, and effective methodologies have been devised to deal with the aforementioned problems. More recently, an alternative technique for underwater vehicle localization has attracted considerable attention: range-only (also called single-beacon)-based localization, whereby the position of an AUV is estimated using discrete measurements of the ranges between the vehicle and a transponder fixed

at a known location, while the AUV undergoes persistently exciting spatial maneuvers.

Previous work on single-beacon acoustic navigation can be traced back to [2], where a least-squares algorithm is proposed to compute the unknown initial position and constant speed of an AUV moving in the horizontal plane, subjected to an unknown constant current. The key concepts behind single-beacon navigation can also be found in [3], which describes a synthetic LBL system based on the combination of dead-reckoning (DR) and acoustic range and/or range rate measurements from a single acoustic source, e.g., a transponder moored to the sea floor. Further relevant work can also be found in [4], where an extended Kalman filter (EKF) for single-beacon navigation is described. In [5], by combining DR data with measurements of the ranges between an underwater vehicle and a single beacon, taken at successive instants of time, a robust estimation algorithm is proposed for vehicle localization in the presence of unknown ocean currents. In [6], a method is described for precise post-processed localization of a deep-diving AUV using only a set of acoustic ranges from a surface ship, while the AUV executes a closed path under the ship. The approach is validated through the experimental results with the Autosub 6000 AUV. For a concise and thorough presentation of previous work in the field and the description of a novel algorithm for single-beacon one-way-travel-time acoustic navigation for underwater vehicles, the reader is referred to [7] and [8], and the references therein.

Some of the most recent solutions proposed for range-based localization borrow from the concept of simultaneous localization and mapping (SLAM) that was first advanced in the field of mobile robots. The key idea of SLAM is to build a new map, or update an existing map of the environment, while at the same time localizing a robot within that map. Pioneering work in this area is described in [9], where a pure range-only subsea SLAM approach is described for AUV localization. The authors assume that the AUV is equipped with a conventional LBL transceiver that measures the acoustic times of flight between the vehicle and a set of submerged transponders. Using only range data and no prior information other than the approximate water column depth, they present a methodology to compute both the transponder locations and the vehicle trajectories (see also [10], where a range-only simultaneous AUV and beacon localization system that assumes no prior knowledge of the beacons' locations and is robust against sensor noise and acoustic outliers is presented). More recently, Petillot *et al.* [11] have proposed a range-only system for underwater vehicle localization that is based on a particle-filtering implementation of SLAM, coupled with a mixture-of-Gaussians representation of the posterior distribution of the beacons' positions.

No matter what particular algorithm is chosen for vehicle localization, a crucial and often forgotten issue is that of ascertaining the observability properties of the design model adopted. In the absence of observability, the attempt to design a localization system will be destined to fail. For this reason, it is important to find conditions under which the design model of a range-based localization systems is observable. Examples of observability studies include [12], where a necessary and sufficient condition for local observability of a 2D maneuvering target tracking system with range-only measurements is derived using estimation-theoretic methods. Historically, one of the first formal studies of observability of single-beacon AUV localization is described in [13] and [14], where linearization techniques and classical tools of linear time-invariant observability analysis are used. A different strategy is used in [15] and [16] to study the observability of a range-based localization system by considering an equivalent augmented linear time varying (LTV) and resorting to LTV system analysis tools (see also the approach in [16] for an interesting related study in a discrete-time, uniform sampling setting). Yet another approach is described in [17], where the problem of relative AUV localization using intervehicle range measurements was studied by exploiting tools from nonlinear observability theory. The results obtained are validated experimentally in an equivalent single-beacon navigation scenario. In spite of substantial progress made in this area, however, work is still required to explicitly characterize the types of AUV trajectories that yield observability of range-based localization systems.

Motivated by the above considerations, the first part of this paper addresses the key observability issues pertaining to the problem of range-based AUV localization using single and multiple fixed beacons, in the presence of constant unknown ocean currents. We explicitly consider the case where the positions of the beacons may be unknown, and thus require that they be localized as well. To this effect, we start by applying a coordinate transformation similar to the one presented in [18], implying a state augmentation that yields a state-affine system with algebraic constraints. We then establish, for the important case where the motion of the AUV is characterized by constant linear and angular velocities expressed in the body frame (that is, trimming trajectories), conditions for which it is possible to reconstruct the initial state of the resulting system. The latter includes the position of the AUV as well as the positions of the beacons. In the analysis, we borrow from the nomenclature and the mathematical concepts of nonlinear system observability introduced in [19]. We show, under some reasonable practical conditions restricted to the assumption that the position of at least one of the beacons or the initial position of the AUV is known, that the localization system is at least weakly observable, meaning that the set of indistinguishable initial states is composed by a set of finite isolated points. By adding depth measurements or allowing the vehicle to undergo motion along the concatenation of at least two trimming trajectories, the resulting system becomes observable, in the sense that the set of indistinguishable points reduces to a singleton.

The key novel contributions that emerge from the first part of this paper are the following.

i) We derive conditions for the observability of the simultaneous AUV/beacon localization system in terms of AUV motion characteristics that are naturally expressed in the body frame and are therefore extremely easy to interpret.
ii) We address the case where the location and number of the beacons may be unknown and vary over time.

iii) We explicitly assume that the state of the system under consideration evolves continuously in time, but that the measurements occur at discrete times and the sampling time need not be constant (i.e., the measurement process is event driven).

iv) Finally, the above issues are tackled by assuming that there may be unknown but constant currents. Previous related work on the issue of observability in the absence of currents and assuming continuous time measurements can be found in [20].

The second part of this paper addresses the problem of range-based localization system design. We exploit the observability properties derived in the first part of this paper and use the concepts of minimum-energy (ME) estimation, projection filters (PFs), and multiple-model estimation techniques, to derive a novel observer that solves the AUV localization problem using relative range measurements to stationary beacons, the locations of which may also be unknown. In contrast to a number of results described in the literature, we give conditions under which the AUV and beacon estimation errors converge to a small neighborhood of zero (whose size depends on the magnitude of the process/measurement noise). The rationale behind the use of the techniques adopted stems from the following facts.

i) We resort to ME observers in a deterministic setting because, as will become clear latter, for the localization problem at hand, it is not natural to assume that the state and observation noise are stochastic processes with Gaussian distributions. This is in striking contrast to the assumptions that are at the root of Kalman filter designs in a stochastic setting. We remind the reader that an ME observer is an optimal filter that produces an estimate of the state of a system that is most compatible with the system dynamics and measured outputs for the lowest possible energy of the state and observation noise signals [21]. For linear systems, ME observers yield a structure akin to that of Kalman filters, albeit in a fully deterministic framework (see [18] for the derivation of an ME estimator for linear dynamic systems with perspective outputs). The deterministic setup adopted affords us an expedite manner to assess the convergence properties of the proposed estimator in terms of bounds on the magnitude of the process and measurement noise.

ii) The state-affine design model that we develop has the interesting property that the state must satisfy a set of quadratic constraints. To explicitly address these constraints, we exploit the techniques proposed in [21] to solve the problem of ME state estimation for systems with perspective outputs and state constraints. They naturally lead to a PF that significantly improves the performance of the proposed observer.

iii) Localizing the beacons naturally arises from the fact that we are also interested in estimating the location of the subset of beacons whose number and positions may be unknown.

iv) Finally, the multiple-model approach adopted allows us to explicitly address the fact that, according to the observability results obtained, there may be distinct AUV trajectories (generated by the same input) corresponding to multiple isolated initial conditions that will yield the same output time histories.

The efficacy of the proposed observer structure is validated through real-world field experiments using the MEDUSA-class of autonomous marine robotic vehicles equipped with ranging devices. In the experiments, one of the vehicles plays the role of an AUV, while the other two serve as proxies for underwater beacons.

This paper is organized as follows. Section II derives the model underlying the design of a range-based localization system with single or multiple beacons. The observability analysis of the proposed design model is done in Section III. Section IV derives the observer that is used to estimate the states of the system and discusses its convergence properties in Section V. Section VI describes the experimental results with a set of marine vehicles that show the efficacy of the nonlinear observer and illustrate the implications of the observability conditions derived. The conclusions are given in Section VII. *All the proofs of the theorems in Section III are presented in the Appendix.*

II. PROCESS MODEL

This section introduces the model adopted to design an AUV localization system that relies on the computation of the ranges between the vehicle and one or more underwater beacons, the location of which may be unknown. The objective is to compute in real time an estimate of the position of the AUV and simultaneously construct a map composed by the estimates of the locations of the beacons. We consider that the AUV motion is subjected to the influence of unknown but constant ocean currents. In what follows, we introduce two coordinate frames: 1) an earth-fixed or inertial coordinate frame $\{\mathcal{I}\}$ and 2) a body-fixed coordinate frame $\{\mathcal{B}\}$ that is attached to the AUV and moves with it. We let $({}^{\mathcal{I}}\boldsymbol{p}_{\mathcal{B}}, {}^{\mathcal{I}}_{\mathcal{B}}\mathcal{R}) \in \mathbb{R}^3 \times \mathrm{SO}(3)$ be the configuration of frame $\{\mathcal{B}\}$ with respect to $\{\mathcal{I}\}$, where ${}^{\mathcal{I}}\boldsymbol{p}_{\mathcal{B}}$ is the position of the AUV in frame $\{\mathcal{I}\}$ and ${}^{\mathcal{I}}_{\mathcal{B}}\mathcal{R}$ is the rotation matrix from $\{\mathcal{B}\}$ to $\{\mathcal{I}\}$. We denote by SO(3) the group of special orthogonal matrices in 3D space. With this notation, the kinematic equations of motion of the AUV can be written as

$$ {}^{\mathcal{I}}\dot{\boldsymbol{p}}_{\mathcal{B}} = {}^{\mathcal{I}}_{\mathcal{B}}\mathcal{R}\,\boldsymbol{v} + {}^{\mathcal{I}}\boldsymbol{v}_c \tag{1} $$

$$ {}^{\mathcal{I}}_{\mathcal{B}}\dot{\mathcal{R}} = {}^{\mathcal{I}}_{\mathcal{B}}\mathcal{R}\,S(\boldsymbol{\omega}) \tag{2} $$

$$ {}^{\mathcal{I}}\dot{\boldsymbol{v}}_c = \boldsymbol{0} \tag{3} $$

where $\boldsymbol{v}$ and $\boldsymbol{\omega}\colon [0,\infty) \to \mathbb{R}^3$ denote the body-fixed linear and angular velocities of the AUV, respectively, relative to $\{\mathcal{I}\}$, expressed in $\{\mathcal{B}\}$, ${}^{\mathcal{I}}\boldsymbol{v}_c \in \mathbb{R}^3$ is an unknown constant ocean current in $\{\mathcal{I}\}$, and for every $a \in \mathbb{R}^3$

$$ S(\boldsymbol{a}) := \begin{bmatrix} 0 & -a_3 & a_2 \\ a_3 & 0 & -a_1 \\ -a_2 & a_1 & 0 \end{bmatrix} $$

is the skew-symmetric matrix representing the linear map $a \mapsto a \times b$, $b \in \mathbb{R}^3$, where $\times$ is the standard cross product in $\mathbb{R}^3$.

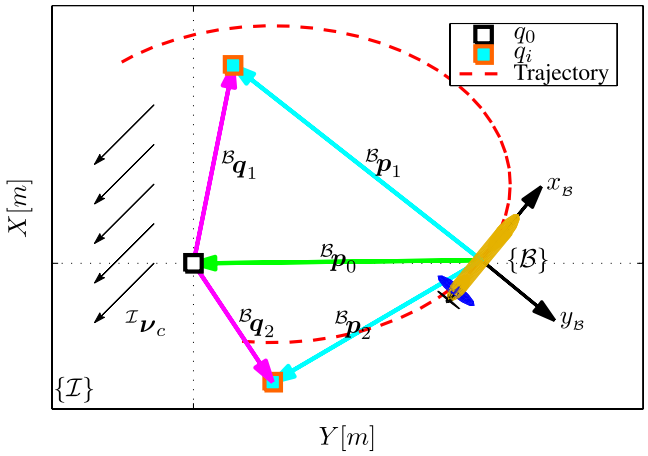

Fig. 1. Illustration of representative state vectors in 2D space.

In what follows, we will treat the linear and angular velocities $\boldsymbol{\nu}$ and $\boldsymbol{\omega}$ as inputs to systems (1)–(3) and use the Euler angle vector $\boldsymbol{\eta} = [\phi, \theta, \psi] \in [0, 2\pi) \times (-(\pi/2), (\pi/2)) \times [0, 2\pi)$ to parameterize the rotation matrix ${}^\mathcal{I}_\mathcal{B}\mathcal{R}$ locally. For simplicity, we denote $c\theta := \cos\theta$ and $s\theta := \sin\theta$. Let $n \in \mathbb{N}$ be the number of stationary beacons q_i located at ${}^\mathcal{I}\boldsymbol{q}_i = [x_i, y_i, z_i]' \in \mathbb{R}^3$, $i \in \{1, 2, \ldots, n\}$, which we assume are not known, with the exception of their depth coordinates z_i. Clearly

$$ {}^\mathcal{I}\dot{\boldsymbol{q}}_i = 0. \tag{4} $$

For each $i \in \{1, 2, \ldots, n\}$, let $r_i(t)$ be the acoustic-based measurement of the range between the AUV and the ith beacon, acquired at time $t \geq 0$. Assuming that the depth z_0 of the AUV can be measured, the measurement/output model that we adopt can be written as

$$ r_i = \left\| {}^\mathcal{I}\boldsymbol{q}_i - {}^\mathcal{I}\boldsymbol{p}_\mathcal{B} \right\| \tag{5} $$

$$ z_i = \boldsymbol{e}_z' {}^\mathcal{I}\boldsymbol{q}_i \tag{6} $$

$$ z_0 = \boldsymbol{e}_z' {}^\mathcal{I}\boldsymbol{p}_\mathcal{B} \tag{7} $$

where $\boldsymbol{e}_x = [1, 0, 0]'$, $\boldsymbol{e}_y = [0, 1, 0]'$, and $\boldsymbol{e}_z = [0, 0, 1]'$.

Equations (1)–(7) represent the nonlinear continuous model of the multiple beacon–AUV localization problem that we address in this paper. In the sequel, for observability analysis purposes, we will construct a state-affine system and derive conditions under which this new system is *equivalent* to (1)–(7), in the sense that there is a one-to-one correspondence between the state trajectories of the original nonlinear system and the newly constructed one. We remark that the strategy adopted to obtain the equivalent state-affine system does not follow the ones described in [22] and [23], but is instead tailored to our specific application. The key ideas exploited are to express the positions of the beacons q_i in the body frame $\{\mathcal{B}\}$ and to introduce a *virtual* beacon, q_0, located at an arbitrary point that we take as the origin of the inertial frame $\{\mathcal{I}\}$ (Fig. 1). Following this strategy and exploiting some of the concepts presented in [18], we define:

$$ {}^\mathcal{B}\boldsymbol{p}_i = {}^\mathcal{I}_\mathcal{B}\mathcal{R}' {}^\mathcal{I}\boldsymbol{q}_i - {}^\mathcal{I}_\mathcal{B}\mathcal{R}' {}^\mathcal{I}\boldsymbol{p}_\mathcal{B} \qquad i \in \{0, 1, \ldots, n\} \tag{8} $$

as the vector directed from the vehicle to beacon q_i expressed in $\{\mathcal{B}\}$. From (1), (2), and (4), it follows that:

$$ \begin{aligned} {}^\mathcal{B}\dot{\boldsymbol{p}}_i &= {}^\mathcal{I}_\mathcal{B}\dot{\mathcal{R}}' \left({}^\mathcal{I}\boldsymbol{q}_i - {}^\mathcal{I}\boldsymbol{p}_\mathcal{B} \right) + {}^\mathcal{I}_\mathcal{B}\mathcal{R}' {}^\mathcal{I}\dot{\boldsymbol{q}}_i - {}^\mathcal{I}_\mathcal{B}\mathcal{R}' {}^\mathcal{I}\dot{\boldsymbol{p}}_\mathcal{B} \\ &= -S(\boldsymbol{\omega}) {}^\mathcal{B}\boldsymbol{q}_i - \boldsymbol{\nu} - {}^\mathcal{B}\boldsymbol{\nu}_c. \end{aligned} $$

Using (2) and the equalities ${}^\mathcal{B}\boldsymbol{\nu}_c = {}^\mathcal{I}_\mathcal{B}\mathcal{R}' {}^\mathcal{I}\boldsymbol{\nu}_c$ and ${}^\mathcal{B}\boldsymbol{q}_i = {}^\mathcal{I}_\mathcal{B}\mathcal{R}' {}^\mathcal{I}\boldsymbol{q}_i$, it can be verified that

$$ {}^\mathcal{B}\dot{\boldsymbol{\nu}}_c = -S(\boldsymbol{\omega}) {}^\mathcal{B}\boldsymbol{\nu}_c, \quad {}^\mathcal{B}\dot{\boldsymbol{q}}_i = -S(\boldsymbol{\omega}) {}^\mathcal{B}\boldsymbol{q}_i. $$

Furthermore, from (8) and the fact that ${}^\mathcal{B}\boldsymbol{q}_i = {}^\mathcal{B}\boldsymbol{p}_i - {}^\mathcal{B}\boldsymbol{p}_0$, the range measurement equation (5) can be written as

$$ r_i = \left\| {}^\mathcal{I}\boldsymbol{q}_i - {}^\mathcal{I}\boldsymbol{p}_\mathcal{B} \right\| = \left\| {}^\mathcal{I}_\mathcal{B}\mathcal{R} {}^\mathcal{B}\boldsymbol{q}_i \right\| = \left\| {}^\mathcal{B}\boldsymbol{q}_i + {}^\mathcal{B}\boldsymbol{p}_0 \right\| $$

where the last equality follows from the fact that any rotation matrix is orthogonal.

To make (5) linear in the state variables, we rewrite it as $r_i = \chi_i$, with $\chi_i := \| {}^\mathcal{B}\boldsymbol{q}_i + {}^\mathcal{B}\boldsymbol{p}_0 \|$ viewed as a new extra state variable. Straightforward computations yield

$$ \dot{\chi}_i = -\left(\boldsymbol{\nu}' \left({}^\mathcal{B}\boldsymbol{q}_i + {}^\mathcal{B}\boldsymbol{p}_0 \right) + {}^\mathcal{B}\boldsymbol{\nu}_c' \left({}^\mathcal{B}\boldsymbol{q}_i + {}^\mathcal{B}\boldsymbol{p}_0 \right) \right) \Big/ r_i. \tag{9} $$

Note that (9) is not valid when $r_i = 0$, which corresponds to the particular case where the position of the AUV coincides with the location of the ith beacon. To avoid this singularity (in particular, at the observer design stage), one possible simple solution is to add a small term $\epsilon > 0$ to r_i in (9). This term can be a function of r_i and must be defined so as to be nonzero when $r_i = 0$. From a practical point of view, this issue can be avoided by preventing the vehicle's position to coincide with one of the positions of the beacons. For example, by positioning the latter at depths different from those where the AUV is expected to operate. Note also that (9) contains nonlinear terms such as the products of state variables. To deal with this fact, we introduce an additional set of $n+1$ state variables. Define $\chi_c := {}^\mathcal{B}\boldsymbol{\nu}_c' {}^\mathcal{B}\boldsymbol{\nu}_c$, and for each $i \in \{1, \ldots, n\}$, let $\chi_{c_i} := {}^\mathcal{B}\boldsymbol{\nu}_c' ({}^\mathcal{B}\boldsymbol{q}_i + {}^\mathcal{B}\boldsymbol{p}_0)$. Straightforward computations show that

$$ \begin{aligned} \dot{\chi}_i &= -\left(\boldsymbol{\nu}' \left({}^\mathcal{B}\boldsymbol{q}_i + {}^\mathcal{B}\boldsymbol{p}_0 \right) + \chi_{c_i} \right) \Big/ r_i \\ \dot{\chi}_{c_i} &= {}^\mathcal{B}\boldsymbol{\nu}_c' S(\boldsymbol{\omega}) {}^\mathcal{B}\boldsymbol{p}_0 - {}^\mathcal{B}\boldsymbol{\nu}_c' \left(S(\boldsymbol{\omega}) {}^\mathcal{B}\boldsymbol{p}_0 + \boldsymbol{\nu} + {}^\mathcal{B}\boldsymbol{\nu}_c \right) \\ &\quad + {}^\mathcal{B}\boldsymbol{\nu}_c' S(\boldsymbol{\omega}) {}^\mathcal{B}\boldsymbol{q}_i - {}^\mathcal{B}\boldsymbol{\nu}_c' S(\boldsymbol{\omega}) {}^\mathcal{B}\boldsymbol{q}_i = -\boldsymbol{\nu}' {}^\mathcal{B}\boldsymbol{\nu}_c - \chi_c \\ \dot{\chi}_c &= {}^\mathcal{B}\boldsymbol{\nu}_c' S(\boldsymbol{\omega}) {}^\mathcal{B}\boldsymbol{\nu}_c - {}^\mathcal{B}\boldsymbol{\nu}_c' S(\boldsymbol{\omega}) {}^\mathcal{B}\boldsymbol{\nu}_c = 0. \end{aligned} $$

Using the equalities ${}^\mathcal{I}\boldsymbol{q}_i = {}^\mathcal{I}_\mathcal{B}\mathcal{R} {}^\mathcal{B}\boldsymbol{q}_i$ and ${}^\mathcal{I}\boldsymbol{p}_\mathcal{B} = -{}^\mathcal{I}_\mathcal{B}\mathcal{R} {}^\mathcal{B}\boldsymbol{p}_0$, (6) and (7) can be written as

$$ z_i = \boldsymbol{e}_z' {}^\mathcal{I}_\mathcal{B}\mathcal{R} {}^\mathcal{B}\boldsymbol{q}_i, \quad z_0 = -\boldsymbol{e}_z' {}^\mathcal{I}_\mathcal{B}\mathcal{R} {}^\mathcal{B}\boldsymbol{p}_0. $$

Putting together the above equations, we obtain a state-affine system with state vector $\boldsymbol{x} \in \mathbb{R}^{5n+7}$, input vector $\boldsymbol{u} \in \mathbb{R}^9$, and output vector $\boldsymbol{y} \in \mathbb{R}^{2n+1}$, described by

$$ \begin{cases} \dot{\boldsymbol{x}}(t) = A_{\boldsymbol{u},\boldsymbol{y}}(t)\boldsymbol{x}(t) + \boldsymbol{b}_{\boldsymbol{u}}(t) \\ \boldsymbol{y}(t) = C_{\boldsymbol{u}}(t)\boldsymbol{x}(t) \end{cases} \tag{10} $$

where

$$\boldsymbol{x} := \Big[{}^{\mathcal{B}}\boldsymbol{p}_0',\ \Big[{}^{\mathcal{B}}\boldsymbol{q}_1' \dots\ {}^{\mathcal{B}}\boldsymbol{q}_n'\Big], {}^{\mathcal{B}}\boldsymbol{v}_c',\ \chi_c, \big[\chi_{c_1}\ \dots\ \chi_{c_n}\big], \big[\chi_1\ \dots\ \chi_n\big]\Big]'$$

$$\boldsymbol{u} := [\,\boldsymbol{v}'\ \ \boldsymbol{\omega}'\ \ \boldsymbol{\eta}'\,]'$$

$$\boldsymbol{y} := [[r_1\ \dots\ r_n],\ z_0,\ [\,z_1\ \dots\ z_n\,]]'$$

$$\boldsymbol{s} := \Big[\frac{1}{r_1}\ \ \frac{1}{r_2}\ \ \dots\ \ \frac{1}{r_n}\Big]',\quad \Omega := S(\boldsymbol{\omega})$$

$$A_{\boldsymbol{u},\boldsymbol{y}} := -\begin{bmatrix} \Omega & \mathbf{0} & I_3 & \mathbf{0} & \mathbf{0} & \mathbf{0} \\ \mathbf{0} & I_n \otimes \Omega & \mathbf{0} & \mathbf{0} & \mathbf{0} & \mathbf{0} \\ \mathbf{0} & \mathbf{0} & \Omega & \mathbf{0} & \mathbf{0} & \mathbf{0} \\ \mathbf{0} & \mathbf{0} & \mathbf{0} & 0 & \mathbf{0} & \mathbf{0} \\ \mathbf{0} & \mathbf{0} & \mathbf{1}_n \otimes \boldsymbol{v}' & \mathbf{1}_n & \mathbf{0} & \mathbf{0} \\ \boldsymbol{s} \otimes \boldsymbol{v}' & \mathrm{diag}(\boldsymbol{s}) \otimes \boldsymbol{v}' & \mathbf{0} & \mathbf{0} & \mathrm{diag}(\boldsymbol{s}) & \mathbf{0} \end{bmatrix}$$

$$\boldsymbol{b}_{\boldsymbol{u}} := \begin{bmatrix} -\boldsymbol{v} \\ \mathbf{0} \\ \mathbf{0} \\ \mathbf{0} \\ \mathbf{0} \\ \mathbf{0} \end{bmatrix}$$

$$C_{\boldsymbol{u}} := \begin{bmatrix} \mathbf{0} & \mathbf{0} & \mathbf{0} & \mathbf{0} & \mathbf{0} & I_n \\ -\boldsymbol{e}_{z\mathcal{B}}'^{\mathcal{I}}\mathcal{R}(\boldsymbol{\eta}) & \mathbf{0} & \mathbf{0} & 0 & \mathbf{0} & \mathbf{0} \\ \mathbf{0} & I_n \otimes \big(\boldsymbol{e}_{z\mathcal{B}}'^{\mathcal{I}}\mathcal{R}(\boldsymbol{\eta})\big) & \mathbf{0} & \mathbf{0} & \mathbf{0} & \mathbf{0} \end{bmatrix}$$

that satisfies the following quadratic constraints for each $i \in \{1, 2, \dots, n\}$:

$$\chi_i^2 = \big\|{}^{\mathcal{B}}\boldsymbol{q}_i + {}^{\mathcal{B}}\boldsymbol{p}_0\big\|^2 \tag{11}$$

$$\chi_c = \big\|{}^{\mathcal{B}}\boldsymbol{v}_c\big\|^2 \tag{12}$$

$$\chi_{c_i} = {}^{\mathcal{B}}\boldsymbol{v}_c'\big({}^{\mathcal{B}}\boldsymbol{q}_i + {}^{\mathcal{B}}\boldsymbol{p}_0\big). \tag{13}$$

In the above model, we have used the following notation: given $M_1, M_2 \in \mathbb{R}^{m_i \times n_i}$ and $\boldsymbol{v} \in \mathbb{R}^n$, we denote by $M_1 \otimes M_2 \in \mathbb{R}^{m_1 n_1 \times m_2 n_2}$ the Kronecker product of M_1 by M_2 and by $\mathrm{diag}(\boldsymbol{v})$ the diagonal $n \times n$ matrix with its main diagonal given by $\boldsymbol{v}$. Moreover, $\mathbf{0}$, $\mathbf{1}_n$, and I_n denote a zero matrix of appropriate dimension, a column vector of ones with length n, and the identity matrix of size n, respectively.

Note that for any trajectory in the state space of the original system (1)–(3), there is a unique corresponding trajectory in the augmented state space of system (10). Conversely, combining the quadratic constraints (11)–(13) with the state-affine system (10) guarantees that every trajectory of (10) has a corresponding state-space trajectory in (1)–(3). Once an equivalent state-affine system is obtained, one can resort to powerful tools of linear systems theory for observability analysis.

An important problem that needs to be addressed explicitly is the fact that due to practical limitations, range/depth measurements are only available at discrete instants of time. This has direct impact on the observability of the underlying model as well as on the performance of a corresponding observer. Furthermore, the observations may not even be periodic due to the fact that the times taken by acoustic waves to travel between the beacons and the AUV will depend on their relative positions. To accommodate these issues, we adopt the following model with continuous-time state dynamics and discrete observations:

$$\begin{cases} \dot{\boldsymbol{x}}(t) = A_{\boldsymbol{u},\boldsymbol{y}}(t)\boldsymbol{x}(t) + \boldsymbol{b}_{\boldsymbol{u}}(t) \\ \boldsymbol{y}(t_k) = C_{\boldsymbol{u}}(t_k)\boldsymbol{x}(t_k) \end{cases} \tag{14}$$

where the possible nonuniform times t_k, $k \in \{0, 1, 2, \dots\}$, are the instants at which range/depth measurements are acquired on board the AUV.

III. Observability Analysis

This section addresses the observability of the model introduced in Section II. In particular, given the dynamical system (14) with unknown initial condition $\boldsymbol{x}(t_0) = \boldsymbol{x}_0$, subject to (11)–(13), the objective is to determine conditions under which it will be possible to compute $\boldsymbol{x}_0$ from the knowledge of the input/output time histories $\{\boldsymbol{u}(t),\ t \in [t_0, t_f),\ \boldsymbol{y}(t_k),\ t_k \in [t_0, t_f)\}$ for some $t_f > t_0$.

To set the stage for a formal discussion of observability, we first introduce the following definitions adopted from [19] and [24]. Note, however, that in this paper, for observability analysis purposes, we will not adopt the observability conditions derived in [19] for general nonlinear systems. Instead, we will derive specific conditions for the system under study that are simple to characterize in terms of the type of motion imparted to the AUV.

Definition 1: Given the system (14) and a time interval $[t_0, t_f)$, two initial conditions $\boldsymbol{z}$ and $\check{\boldsymbol{z}}$ are said to be indistinguishable on $[t_0, t_f)$ if the output time histories $\{\boldsymbol{y}(t_k),\ t_k \in [t_0, t_f)\}$, resulting from all admissible input time series $\{\boldsymbol{u}(t),\ t \in [t_0, t_f)\}$ and satisfying the initial conditions $\boldsymbol{x}(t_0) = \boldsymbol{z}$ and $\boldsymbol{x}(t_0) = \check{\boldsymbol{z}}$, are identical. For every $\boldsymbol{z}$, $\mathcal{I}(\boldsymbol{z})$ denotes the set of all initial conditions that are indistinguishable from $\boldsymbol{z}$ on $[t_0, t_f)$.

Definition 2: The system (14) is observable at $\boldsymbol{z}$ on $[t_0, t_f)$ if $\mathcal{I}(\boldsymbol{z}) = \{\boldsymbol{z}\}$, and it is observable on $[t_0, t_f)$ if $\mathcal{I}(\boldsymbol{z}) = \{\boldsymbol{z}\}$ for every $\boldsymbol{z}$.

Definition 3: The system (14) is weakly observable at $\boldsymbol{z}$ on $[t_0, t_f)$ if $\boldsymbol{z}$ is an isolated point of $\mathcal{I}(\boldsymbol{z})$, and it is weakly observable on $[t_0, t_f)$ if it is weakly observable for every $\boldsymbol{z}$.

Note that weak observability at a point $\boldsymbol{z}$ does not imply that every input from the class $\mathcal{U}_{\mathrm{ad}}$ of admissible inputs will distinguish $\boldsymbol{z}$ from any other state in a small neighborhood of $\boldsymbol{z}$. Different inputs may be required to distinguish $\boldsymbol{z}$ from other states in that neighborhood. For this reason, the notion of observability defined above, even though elegant, may not be entirely satisfactory in a number of applications. Interestingly enough, in some engineering problems dealing with autonomous vehicles, there exist reduced classes $\mathcal{U}_c \subseteq \mathcal{U}_{\mathrm{ad}}$ of admissible input signals named $\boldsymbol{u}^*$, sufficiently general to yield maneuvers of interest in a wide range of applications, and yet restricted in the sense that they can be easily parameterized in terms of a small number of parameters with a strong physical interpretation. Such is the case with AUVs when they undergo motion along trimming trajectories (generated by holding the input actuators fixed) that are easily parameterized by total speed, yaw rate, and flight path angle and correspond to helices in 3D space that may degenerate into circumferences and straight lines [25]. In these cases, it is of interest to a

practitioner to ascertain the observability properties of a given system for a reduced class of inputs $\mathcal{U}_c$, rather than allowing for all inputs that are physically admissible. Motivated by these considerations, we introduce a weaker notion of observability originally proposed in [26], which, as we shall see, will allow for the derivation of observability condition for the localization system studied in this paper that are easy to interpret physically.

Definition 4: Given the system (14) and a time interval $[t_0, t_f)$, two initial conditions z and $\check{z}$ are said to be $\boldsymbol{u}^*$-indistinguishable on $[t_0, t_f)$ if the output time histories $\{\boldsymbol{y}(t_k), t_k \in [t_0, t_f)\}$ for an input time series $\{\boldsymbol{u}^*(t) \in \mathcal{U}_c, t \in [t_0, t_f)\}$ satisfying the initial conditions $\boldsymbol{x}(t_0) = z$ and $\boldsymbol{x}(t_0) = \check{z}$ are identical. For every z, $\mathcal{I}^{\boldsymbol{u}^*}(z)$ denotes the set of all initial conditions that are $\boldsymbol{u}^*$-indistinguishable from z on $[t_0, t_f)$.

Definition 5: Given $\boldsymbol{u}^* \in \mathcal{U}_c$ and a time interval $[t_0, t_f)$, the system (14) is $\boldsymbol{u}^*$-observable at z on $[t_0, t_f)$ if $\mathcal{I}^{\boldsymbol{u}^*}(z) = \{z\}$, and is $\boldsymbol{u}^*$-observable on $[t_0, t_f)$ if $\mathcal{I}^{\boldsymbol{u}^*}(z) = \{z\}$ for every z.

Definition 6: Given $\boldsymbol{u}^* \in \mathcal{U}_c$ and a time interval $[t_0, t_f)$, the system (14) is $\boldsymbol{u}^*$-weakly observable at z on $[t_0, t_f)$ if z is an isolated point of $\mathcal{I}^{\boldsymbol{u}^*}(z)$ and is $\boldsymbol{u}^*$-weakly observable on $[t_0, t_f)$ if it is $\boldsymbol{u}^*$-weakly observable for every z.

Note that observability implies weak observability, and $\boldsymbol{u}^*$-observability implies $\boldsymbol{u}^*$-weak observability. Throughout this paper, we will use the weaker notions of observability. To simplify the terminology, we shall often abbreviate the nomenclature of $\boldsymbol{u}^*$-indistinguishable, $\boldsymbol{u}^*$-observable, and $\boldsymbol{u}^*$-weakly observable to indistinguishable, observable, and weakly observable, respectively.

We now define formally the class of admissible inputs $\boldsymbol{u} \in \mathcal{U}_c$ that we consider for the system described by (14). To this effect, as explained before, we restrict ourselves to AUV trimming (also called equilibrium or steady state) trajectories. Straightforward computations similar to those in [25] done for the case of aircraft show that at trimming

$$\boldsymbol{\omega}_e = \dot{\psi}_e [\, -s\theta_e \quad s\phi_e c\theta_e \quad c\phi_e c\theta_e \,]' = \dot{\psi}_e \, {}^{\mathcal{I}}_{\mathcal{B}}\mathcal{R}'(\boldsymbol{\eta}_e)\, \boldsymbol{e}_z \quad (15)$$

where the subscript e denotes the value of a variable at steady state, and $\phi(t) = \phi_e$, $\theta(t) = \theta_e$, and $\dot{\psi}_e$ are the values of roll angle, pitch angle, and yaw rate, respectively, at steady state.

For clarity of exposition, the observability analysis will be first carried out for the case of one beacon only, that is, $n = 1$. We will also work with the states χ_1^2 and r_1^2 (squared range output) instead of χ_1 and r_1, respectively. With these assumptions, (14) yields

$$\begin{cases} \dot{\boldsymbol{x}}(t) = A_{\boldsymbol{u}}(t)\boldsymbol{x}(t) + \boldsymbol{b}_{\boldsymbol{u}}(t) \\ \boldsymbol{y}(t_k) = C_{\boldsymbol{u}}(t_k)\boldsymbol{x}(t_k) \end{cases} \quad (16)$$

where $\boldsymbol{x} := [\, {}^{\mathcal{B}}\boldsymbol{p}_0' \; {}^{\mathcal{B}}\boldsymbol{q}_1' \; {}^{\mathcal{B}}\boldsymbol{v}_c' \; \chi_c \; \chi_{c_1} \; \chi_1^2 \,]'$, $\boldsymbol{y} := [\, r_1^2 \; z_0 \; z_1 \,]'$, $\boldsymbol{u} := [\, \boldsymbol{v}_e' \; \boldsymbol{\omega}_e' \; \phi_e \; \theta_e \,]'$, and

$$A_{\boldsymbol{u}} := -\begin{bmatrix} \Omega_e & \mathbf{0} & I_3 & \mathbf{0} & \mathbf{0} & \mathbf{0} \\ \mathbf{0} & \Omega_e & \mathbf{0} & \mathbf{0} & \mathbf{0} & \mathbf{0} \\ \mathbf{0} & \mathbf{0} & \Omega_e & \mathbf{0} & \mathbf{0} & \mathbf{0} \\ \mathbf{0} & \mathbf{0} & \mathbf{0} & 0 & 0 & 0 \\ \mathbf{0} & \mathbf{0} & \boldsymbol{v}_e' & 1 & 0 & 0 \\ 2\boldsymbol{v}_e' & 2\boldsymbol{v}_e' & \mathbf{0} & 0 & 2 & 0 \end{bmatrix}, \quad \boldsymbol{b}_{\boldsymbol{u}} := \begin{bmatrix} -\boldsymbol{v}_e \\ \mathbf{0} \\ \mathbf{0} \\ \mathbf{0} \\ \mathbf{0} \\ \mathbf{0} \end{bmatrix}$$

$$C_{\boldsymbol{u}} := \begin{bmatrix} 0 & 0 & 0 & 0 & 0 & 0 & \mathbf{0} & 1 \\ s\theta_e & -s\phi_e c\theta_e & -c\phi_e c\theta_e & 0 & 0 & 0 & \mathbf{0} & 0 \\ 0 & 0 & 0 & -s\theta_e & s\phi_e c\theta_e & c\phi_e c\theta_e & \mathbf{0} & 0 \end{bmatrix}.$$

At this point, it is important to note that working with the square of the ranges rather than the ranges themselves does not change the observability results. Suppose, for example, that (16) is $\boldsymbol{u}^*$-observable for a given input $\boldsymbol{u}^*$, in the sense that for every pair of distinct initial conditions $(\boldsymbol{x}_0, z_0)$, there exists a time interval $t \in [t^*, t_f]$, $t^* \geq 0$ such that the corresponding squared range outputs are different, that is, $y(t; \boldsymbol{u}^*, \boldsymbol{x}_0) := r_1^2(t; \boldsymbol{u}^*, \boldsymbol{x}_0) \neq y(t; \boldsymbol{u}^*, z_0) := r_1^2(t; \boldsymbol{u}^*, z_0)$. Then, it also follows that $r_1(t; \boldsymbol{u}^*, \boldsymbol{x}_0) \neq r_1(t; \boldsymbol{u}^*, z_0)$, which implies that the initial conditions $(\boldsymbol{x}_0, z_0)$ for the original system (using ranges) will produce different outputs. The converse implication holds as well.

In what follows, for simplicity of analysis, we will rewrite the equations in (16) by considering the so-called *flow frame* $\{\mathcal{F}\}$ (also called wind frame in aerodynamics), instead of the body-fixed frame $\{\mathcal{B}\}$. With this change of reference frames, the total velocity vector at trimming is aligned with the x-axis of $\{\mathcal{F}\}$, that is, $\boldsymbol{v}_e = [v_e, 0, 0]'$. As is well known, the transformation from flow frame to body-fixed frame is done using a rotation matrix parameterized by the angles of attack and side-slip, which are constant during a trimming maneuver. As expressed in the flow frame, the body angular velocity is also constant at trimming. Therefore, after straightforward computations, it can be concluded that the single-beacon system using the linear velocity $\boldsymbol{v}$ and the angular velocity $\boldsymbol{\omega}$ expressed in the flow frame take the same form as (16), where in this case, the orientation parameterized by $\boldsymbol{\eta}$ is with respect to $\{\mathcal{F}\}$. Throughout this paper, for simplicity of exposition and to avoid changing of the notation, we continue to adopt the model defined by (16), with the understanding that the variables are expressed in the flow frame.

Returning to the observability problem, one immediate result is that, unless there is an *anchor* that relates relative localization to global (inertial) position, the system (16) is not observable. This is due to the fact that range is a relative measurement. To deal with this problem that arises in any SLAM approach, the idea is to use *a priori* knowledge of the position of one of the beacons/AUV and estimate the other unknown ones. For instance, one practical scenario is to consider that the initial position of the AUV is known, which is feasible if the AUV starts from the surface with GPS. Another approach is to consider that the location of one of the beacons is known. In the sequel, we consider the case where the initial condition of the beacon ${}^{\mathcal{B}}\boldsymbol{q}_1(0)$ is known. Later on, we will investigate the dual case where the initial location of AUV ${}^{\mathcal{B}}\boldsymbol{p}_0(0)$ is known.

Given $\boldsymbol{x}_0 \in \mathbb{R}^{12}$, let $\mathcal{I}_r(\boldsymbol{x}_0)$ denote the set of indistinguishable initial conditions from $\boldsymbol{x}_0$ for the system (16) with range-only measurements. The main result of this section is stated in the next theorem, which characterizes $\mathcal{I}_r(\cdot)$ under some conditions.

Theorem 1: Consider the system (16) with range-only measurement, that is, $C_{\boldsymbol{u}} = [\mathbf{0}, 1]$, subject to constraints (11)–(13). Suppose that $\boldsymbol{\omega}_e = [\omega_{e_x}, \omega_{e_y}, \omega_{e_z}]' \in \mathbb{R}^3$

satisfies

$$\|\boldsymbol{\omega}_e\| > \|\omega_{e_x}\| \tag{17}$$

and the number of available samples of measurements on $[t_0, t_f)$ is at least 7 (that is, $n_r \geq 7$). Moreover, let the interarrival times, $t_{k+1} - t_k$, be strictly positive. Then, for every $\boldsymbol{x}_0 \in \mathbb{R}^{12}$ and almost all interarrival times, the set of all initial conditions that are indistinguishable from $\boldsymbol{x}_0$ on $[t_0, t_f)$ is given by

$$\mathcal{I}_r(\boldsymbol{x}_0) = \left\{ \boldsymbol{x}_0, \boldsymbol{x}_0 + \frac{2}{\boldsymbol{\omega}_e'\boldsymbol{\omega}_e} \begin{bmatrix} -\boldsymbol{\omega}_e\boldsymbol{\omega}_e' \left({}^{\mathcal{B}}\boldsymbol{p}_0(0) + {}^{\mathcal{B}}\boldsymbol{q}_1(0)\right) \\ \mathbf{0} \\ -\boldsymbol{\omega}_e\boldsymbol{\omega}_e'\left({}^{\mathcal{B}}\boldsymbol{v}_c(0) + \boldsymbol{v}_e\right) \\ 2\boldsymbol{v}_e'\boldsymbol{\omega}_e\boldsymbol{\omega}_e'\left({}^{\mathcal{B}}\boldsymbol{v}_c(0) + \boldsymbol{v}_e\right) \\ \boldsymbol{v}_e'\boldsymbol{\omega}_e\boldsymbol{\omega}_e'\left({}^{\mathcal{B}}\boldsymbol{p}_0(0) + {}^{\mathcal{B}}\boldsymbol{q}_1(0)\right) \\ 0 \end{bmatrix} \right\}. \tag{18}$$

Furthermore, in this case, the system (16) subject to constraints (11)–(13) is weakly observable on $[t_0, t_f)$. Consider now the degenerate case where the interarrival times are uniform, that is, $t_{k+1} - t_k = T$ for all $t_k \in [t_0, t_f)$. Then, for all interarrival times except for the zero measure set

$$\{t_k | t_{k+1} - t_k = \kappa\pi \|\boldsymbol{\omega}_e\|^{-1}, t_k \in [t_0, t_f), \kappa \in \mathbb{N}^+\} \tag{19}$$

the set of all initial conditions that are indistinguishable from the given initial condition $\boldsymbol{x}_0 \in \mathbb{R}^{12}$ on $[t_0, t_f)$ is given by (18).

The above theorem allows for a simple geometrical interpretation of the nontrivial point in $\mathcal{I}_r(\boldsymbol{x}_0)$. This stems from the fact that the components of the nontrivial point in $\mathcal{I}_r(\boldsymbol{x}_0)$ given by the AUV position and the ocean current velocity can be written as

$$\begin{aligned} {}^{\mathcal{B}}\breve{\boldsymbol{p}}_0(0) &:= \left(I_3 - 2\|\boldsymbol{\omega}_e\|^{-2}\boldsymbol{\omega}_e\boldsymbol{\omega}_e'\right)\left({}^{\mathcal{B}}\boldsymbol{p}_0(0) + {}^{\mathcal{B}}\boldsymbol{q}_1(0)\right) - {}^{\mathcal{B}}\boldsymbol{q}_1(0) \\ {}^{\mathcal{B}}\breve{\boldsymbol{v}}_c(0) &:= \left(I_3 - 2\|\boldsymbol{\omega}_e\|^{-2}\boldsymbol{\omega}_e\boldsymbol{\omega}_e'\right)\left({}^{\mathcal{B}}\boldsymbol{v}_c(0) + \boldsymbol{v}_e\right) - \boldsymbol{v}_e. \end{aligned}$$

Note that from Rodrigues' rotation formula [27], it follows that $I_3 - 2\|\boldsymbol{\omega}_e\|^{-2}\boldsymbol{\omega}_e\boldsymbol{\omega}_e' = -R(\pi, \boldsymbol{\omega}_e/\|\boldsymbol{\omega}_e\|)$. Geometrically, this represents the rotation of $-({}^{\mathcal{B}}\boldsymbol{p}_0(0) + {}^{\mathcal{B}}\boldsymbol{q}_1(0))$ about the $\boldsymbol{\omega}_e$-axis by π. In other words, ${}^{\mathcal{B}}\breve{\boldsymbol{p}}_0(0)$ is the vector sum of $-{}^{\mathcal{B}}\boldsymbol{q}_1(0)$ and the mirror point of the vector ${}^{\mathcal{B}}\boldsymbol{p}_1(0) = {}^{\mathcal{B}}\boldsymbol{p}_0(0) + {}^{\mathcal{B}}\boldsymbol{q}_1(0)$ with respect to plane orthogonal to $\boldsymbol{\omega}_e$. In particular, when ${}^{\mathcal{B}}\boldsymbol{p}_1(0)$ lies in the plane orthogonal to $\boldsymbol{\omega}_e$, ${}^{\mathcal{B}}\boldsymbol{p}_1(0)$ and its mirror point coincide, thereby removing the ambiguity. This is the case when the AUV moves in a horizontal plane. Thus, the range-only system in 2D is observable since the set of indistinguishable points contains only $\boldsymbol{x}_0$. The above geometric interpretation can be exploited to show that a weakly observable system with a given trimming angular velocity (say $\boldsymbol{\omega}_e = \bar{\boldsymbol{\omega}}_e$) will become observable by instantaneously switching to another noncollinear trimming angular velocity $\boldsymbol{\omega}_e = \breve{\boldsymbol{\omega}}_e$ such that $\bar{\boldsymbol{\omega}}_e \times \breve{\boldsymbol{\omega}}_e \neq \mathbf{0}$. This means that the system can become observable by concatenating appropriately chosen distinct trimming trajectories.

From Theorem 1, we obtain the following result for the particular case where the current is zero or known.

Corollary 1: Consider the system (16) with range-only measurement, subject to constraints (11)–(13), and let all the requirements of Theorem 1 hold. Further assume that either there is no ocean current or ${}^{\mathcal{B}}\boldsymbol{v}_c$ is known. Then, for almost all interarrival times, the system (16) is observable, provided

$$\boldsymbol{\omega}_e'\left({}^{\mathcal{B}}\boldsymbol{v}_c + \boldsymbol{v}_e\right) \neq 0. \tag{20}$$

It is well known that the observability properties of a general nonlinear system depend on a particular actuator–sensor configuration. Furthermore, the introduction of additional sensors has the potential to improve the observability properties of the system. The next result shows that by including depth and range measurements, the system becomes observable. In what follows, $\mathcal{I}_{rz}(\boldsymbol{x})$ denotes the set of indistinguishable states associated with the system (16) with range and depth measurements.

Theorem 2: Consider the system (16) with range and depth measurements. Suppose that $\boldsymbol{\omega}_e \in \mathbb{R}^3$ satisfies (17) and the number of available samples of measurements on $[t_0, t_f)$ is at least 7 (that is, $n_r \geq 7$). Moreover, let the interarrival times, $t_{k+1} - t_k$, be strictly positive. Then, for every $\boldsymbol{x}_0 \in \mathbb{R}^{12}$ and almost all interarrival times, $\mathcal{I}_{rz}(\boldsymbol{x}_0) = \{\boldsymbol{x}_0\}$ and the system is observable on $[t_0, t_f)$.

The following corollary of Theorem 2 follows immediately.

Corollary 2: Consider the system (16), and let all the requirements of Theorem 2 hold. Further, assume that either there is no ocean current or ${}^{\mathcal{B}}\boldsymbol{v}_c$ in known. Then, for almost all interarrival times, the system (16) is observable.

Theorem 1 gives sufficient condition (17) for weak observability of system (16) subject to constraints (11)–(13) with range-only measurements. Further, introducing depth measurements yields observability. This prompts the following question: if condition (17) is not satisfied, then what can be stated about the observability properties of system (16) with range (and depth) measurements? The next result discusses this case.

Theorem 3: Consider the system (16) subject to constraints (11)–(13) and suppose that (17) does not hold. Then, the system subject to constraints (11)–(13) is not observable.

Till now, we have investigated the case where the initial location of the beacon, ${}^{\mathcal{B}}\boldsymbol{q}_1(0)$, is known and the initial position of the AUV, ${}^{\mathcal{B}}\boldsymbol{p}_0(0)$, is unknown. We now consider the dual case, that is, ${}^{\mathcal{B}}\boldsymbol{p}_0(0)$ is known but not the initial position of the beacon. The following result holds.

Theorem 4: Consider the system (16), and constraints (11)–(13), and assume that ${}^{\mathcal{B}}\boldsymbol{p}_0(0)$ is known. Then, (16) has observability properties similar to those obtained for the case where ${}^{\mathcal{B}}\boldsymbol{q}_1(0)$ is known (Theorems 1–3), except that the set of indistinguishable points is given by

$$\mathcal{I}_r(\boldsymbol{x}_0) = \left\{ \boldsymbol{x}_0, \boldsymbol{x}_0 + \frac{2}{\boldsymbol{\omega}_e'\boldsymbol{\omega}_e} \begin{bmatrix} \mathbf{0} \\ -\boldsymbol{\omega}_e\boldsymbol{\omega}_e' \left({}^{\mathcal{B}}\boldsymbol{p}_0(0) + {}^{\mathcal{B}}\boldsymbol{q}_1(0)\right) \\ -\boldsymbol{\omega}_e\boldsymbol{\omega}_e'\left({}^{\mathcal{B}}\boldsymbol{v}_c(0) + \boldsymbol{v}_e\right) \\ 2\boldsymbol{v}_e'\boldsymbol{\omega}_e\boldsymbol{\omega}_e'\left({}^{\mathcal{B}}\boldsymbol{v}_c(0) + \boldsymbol{v}_e\right) \\ \boldsymbol{v}_e'\boldsymbol{\omega}_e\boldsymbol{\omega}_e'\left({}^{\mathcal{B}}\boldsymbol{p}_0(0) + {}^{\mathcal{B}}\boldsymbol{q}_1(0)\right) \\ 0 \end{bmatrix} \right\}. \tag{21}$$

We are now ready to state the main result about system (14), which extends the previous results to more than one beacon.

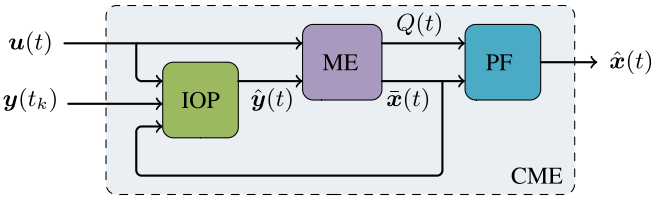

Fig. 2. Block diagram of the CME.

Theorem 5: Consider the system (14) with constant trimming linear velocity $\boldsymbol{v}_e \neq 0$, angular velocity $\boldsymbol{\omega}_e \in \mathbb{R}^3$, and constraints (11)–(13). Suppose that there is an anchor, that is, the initial condition ${}^{\mathcal{B}}\boldsymbol{p}_0(0)$ or the position of one of the beacons ${}^{\mathcal{B}}\boldsymbol{q}_i(0)$ is known. Assume that at least seven samples of measurements, $n_r \geq 7$, are available on $[t_0, t_f)$, and let the interarrival times, $t_{k+1} - t_k$, be strictly positive. Suppose also that (17) holds. Then, for every $\boldsymbol{x}_0 \in \mathbb{R}^{12}$ and almost all interarrival times, the set of all initial conditions that are indistinguishable from $\boldsymbol{x}_0 \in [t_0, t_f)$ is given by $\mathcal{I}_{rz}(\boldsymbol{x}_0) = \{\boldsymbol{x}_0\}$.

Under the same conditions, but with the assumption that only range measurements are available, it follows that the initial condition of each unknown vector in $\{{}^{\mathcal{B}}\boldsymbol{p}_0, {}^{\mathcal{B}}\boldsymbol{q}_i, {}^{\mathcal{B}}\boldsymbol{v}_c; i = 1, 2, \ldots, n\}$ has two possible solutions. Otherwise, if (17) does not hold, then the system subject to constraints (11)–(13) is not observable.

IV. Observer Design

This section addresses the problem of range-based localization system design by taking into consideration the results derived in the previous sections. Consider system (14), corrupted with deterministic but unknown bounded disturbance $\boldsymbol{d} : [0, t] \to \in \mathbb{R}^p$ and measurement noise $\boldsymbol{n}(t_k)$, that is

$$\begin{cases} \dot{\boldsymbol{x}}(t) = A_{\boldsymbol{u},\boldsymbol{y}}(t)\boldsymbol{x}(t) + \boldsymbol{b}_{\boldsymbol{u}}(t) + G_{\boldsymbol{u}}\boldsymbol{d}(t) \\ \boldsymbol{y}(t_k) = C_{\boldsymbol{u}}(t_k)\boldsymbol{x}(t_k) + \boldsymbol{n}(t_k). \end{cases} \tag{22}$$

The goal is to estimate the state vector $\boldsymbol{x}(t)$ given an initial estimate $\hat{\boldsymbol{x}}_0$ and the past control inputs and observations $\{\boldsymbol{u}(\tau), \boldsymbol{y}(t_\tau) : 0 \leq \tau \leq t, t_\tau \in \{t_1, \ldots, t_k\} \subset [0, t]\}$, while satisfying constraints (11)–(13).

To this effect, we propose the observer architecture shown in Fig. 2, which will be henceforth referred to as the constrained ME (CME) observer. The CME is composed of the following subsystems:

- a ME, whose role is to provide an estimate of the state $\bar{\boldsymbol{x}}(t)$ by solving in real time an unconstrained optimization problem (that will be defined later);
- a PF, which maps an unconstrained solution $\bar{\boldsymbol{x}}(t)$ onto a constrained solution $\hat{\boldsymbol{x}}(t)$;
- an intersample output predictor (IOP), which provides a continuous estimate of the range measurement variable to be used by the ME estimator.

Later, we will i) extend the CME observer to deal with the problem of multiple beacons whose number is not known a-priori and can change over time and ii) use the concept of multiple-models to improve the convergence time of the proposed observer by taking into account the observability properties described in the previous sections.

A. Minimum-Energy Estimator

The ME estimator is formulated in a deterministic setting by producing an estimate for the state of the system that is *most compatible* with the system's dynamics and measured outputs. In particular, the optimal state estimate $\bar{\boldsymbol{x}}(t)$ is defined to be the value of the state that is compatible with the observations collected up to time t and the dynamics of the system, for the *lowest* possible measurement noise and disturbance, *lowest* being understood in an integral-square sense [18], [28]. More precisely, the state estimate $\bar{\boldsymbol{x}}$ is obtained from the solution to the optimization problem

$$\bar{\boldsymbol{x}}(t) = \arg \min_{z \in \mathbb{R}^{n_s}} J(z, t)$$

where the cost function $J(\boldsymbol{z}, t)$ is given by

$$\begin{aligned} J(\boldsymbol{z}, t) = \min_{\boldsymbol{d},\boldsymbol{n}} \Bigg\{ & \|\boldsymbol{x}(0) - \bar{\boldsymbol{x}}_0\|_{Q_0} + \int_0^t \|\boldsymbol{d}(\tau)\|^2_{R_{\boldsymbol{d}}^{-1}} d\tau \\ & + \sum_{k=1}^{k^\star} \|\boldsymbol{n}(t_k)\|^2_{R_{\boldsymbol{n}}^{-1}} : \boldsymbol{x}(t) = \boldsymbol{z}, \dot{\boldsymbol{x}} = A_{\boldsymbol{u},\boldsymbol{y}}\boldsymbol{x} + \boldsymbol{b}_{\boldsymbol{u}}(t) \\ & + G_{\boldsymbol{u}}\boldsymbol{d}, \boldsymbol{y}(t_k) = C_{\boldsymbol{u}}\boldsymbol{x}(t_k) + \boldsymbol{n}(t_k) \Bigg\} \end{aligned} \tag{23}$$

with $Q_0 \succ 0$ and the index $k^\star$ satisfying $t_{k^\star} = \lfloor t \rfloor$, where $\lfloor t \rfloor$ denotes the maximum discrete time $t_k \in [0, t)$, which is strictly less than t. The matrices $R_{\boldsymbol{d}}$ and $R_{\boldsymbol{n}} \succ 0$ can be viewed as weighting parameters associated with the disturbances and measurement noises. Using the results in [18], [21], and [28], it can be concluded that this unconstrained state estimation problem has the following exact iterative solution:

- for $t_{k-1} \leq t < t_k, \quad k = 1, \ldots, k^\star$

$$\dot{Q}(t) = -A'_{\boldsymbol{u},\boldsymbol{y}}Q(t) - Q(t)A_{\boldsymbol{u},\boldsymbol{y}} - Q(t)G_{\boldsymbol{u}}R_{\boldsymbol{d}}G'_{\boldsymbol{u}}Q(t) \tag{24}$$

$$\dot{\bar{\boldsymbol{x}}}(t) = A_{\boldsymbol{u},\boldsymbol{y}}\bar{\boldsymbol{x}}(t) + \boldsymbol{b}_{\boldsymbol{u}} \tag{25}$$

- for $t = t_k, \quad k = 1, \ldots, k^\star$

$$Q(t_k) = Q\left(t_k^-\right) + C'_{\boldsymbol{u}}R_{\boldsymbol{n}}^{-1}C_{\boldsymbol{u}} \tag{26}$$

$$\bar{\boldsymbol{x}}(t_k) = \bar{\boldsymbol{x}}\left(t_k^-\right) + Q^{-1}(t_k)C'_{\boldsymbol{u}}R_{\boldsymbol{n}}^{-1}\left(\boldsymbol{y}(t_k) - C_{\boldsymbol{u}}\bar{\boldsymbol{x}}\left(t_k^-\right)\right) \tag{27}$$

while satisfying $Q(0) := Q_0 \succ 0$ and $\bar{\boldsymbol{x}}(0) := \bar{\boldsymbol{x}}_0$.

B. Projection Filter

In general, the solution obtained in the unconstrained state estimation problem $\bar{\boldsymbol{x}}(t)$ does not satisfy constraints (11)–(13). To solve this problem, we first observe that (11)–(13) can be rewritten as quadratic constraints of the form $\boldsymbol{z}'S_i\boldsymbol{z} + \boldsymbol{r}'_i\boldsymbol{z} = 0$, $i \in \{1, \ldots, 2n + 1\}$. Thus, one strategy is to compute $\hat{\boldsymbol{x}}$ such that

$$\hat{\boldsymbol{x}}(t) = \arg \min_{\substack{z \in \mathbb{R}^{n_s}, \\ z'S_l z + \boldsymbol{r}'_l z = 0 \\ \forall l \in \{1, \ldots, 2n+1\}}} (\boldsymbol{z} - \bar{\boldsymbol{x}})'Q(\boldsymbol{z} - \bar{\boldsymbol{x}}). \tag{28}$$

Since (28) does not have a closed-form expression, following the ideas in [21] and [29], we propose a scheme that asymptotically solves the related sufficient Karush–Kuhn–Tucker (KKT) conditions [30, pp. 243 and 244]. More precisely, consider the

Lagrangian function corresponding to the cost function in (28), that is

$$\mathcal{L}(\hat{\boldsymbol{x}}, \boldsymbol{\lambda}) = (\hat{\boldsymbol{x}} - \bar{\boldsymbol{x}})' Q (\hat{\boldsymbol{x}} - \bar{\boldsymbol{x}}) + \sum_{l=1}^{2n+1} \lambda_l (\hat{\boldsymbol{x}}' S_l \hat{\boldsymbol{x}} + \boldsymbol{r}_l' z)$$

where $\boldsymbol{\lambda} \in \mathbb{R}^{2n+1}$ is the Lagrange multiplier vector. This leads to the following sufficient KKT conditions for optimality:

$$\boldsymbol{e}_2 = \bar{Q}\hat{\boldsymbol{x}} - Q\bar{\boldsymbol{x}} + \bar{R}\boldsymbol{\lambda} = \boldsymbol{0}, \quad \boldsymbol{e}_3 = (\bar{S}(\hat{\boldsymbol{x}}) + 2\bar{R})'\hat{\boldsymbol{x}} = \boldsymbol{0} \tag{29}$$

where

$$\bar{S}(\hat{\boldsymbol{x}}) = [S_1\hat{\boldsymbol{x}}, S_2\hat{\boldsymbol{x}}, \ldots, S_{2n+1}\hat{\boldsymbol{x}}]$$
$$\bar{R} = [\boldsymbol{r}_1, \boldsymbol{r}_2, \ldots, \boldsymbol{r}_{2n+1}]/2, \quad \bar{Q} = Q + \sum_{i=1}^{2n+1} \lambda_i S_i. \tag{30}$$

Suppose that along the trajectories of the system, we have that $\bar{Q} \succ 0$ and $\bar{S}(\hat{\boldsymbol{x}}) + \bar{R}$ remain full column rank. Then, setting the initial condition $\hat{\boldsymbol{x}}(0) = \bar{\boldsymbol{x}}_0$, the following proposed solution guarantees that the sufficient KKT conditions for (28) hold at sampling times $t = t_k$ and asymptotically in $[t_{k-1}, t_k)$ (i.e., $\boldsymbol{e}_2$ and $\boldsymbol{e}_3$ converge to zero as t_k goes to infinity):

- for $t_{k-1} \le t < t_k, \quad k = 1, \ldots, k^\star$

$$\begin{bmatrix} \dot{\hat{\boldsymbol{x}}} \\ \dot{\boldsymbol{\lambda}} \end{bmatrix} = \begin{bmatrix} \bar{Q} & \bar{S}(\hat{\boldsymbol{x}}) + \bar{R} \\ \bar{S}(\hat{\boldsymbol{x}})' + \bar{R}' & \boldsymbol{0} \end{bmatrix}^{-1} \left(\begin{bmatrix} -\dot{\bar{Q}}\hat{\boldsymbol{x}} + Q\dot{\bar{\boldsymbol{x}}} + \dot{Q}\bar{\boldsymbol{x}} \\ \boldsymbol{0} \end{bmatrix} - \mu \begin{bmatrix} Q(\hat{\boldsymbol{x}} - \bar{\boldsymbol{x}}) + (\bar{S}(\hat{\boldsymbol{x}}) + \bar{R})\boldsymbol{\lambda} \\ \left(\frac{1}{2}\bar{S}(\hat{\boldsymbol{x}}) + \bar{R}\right)' \hat{\boldsymbol{x}} \end{bmatrix} \right) \tag{31}$$

- for $t = t_k, \quad k = 1, \ldots, k^\star$

$$\begin{bmatrix} \hat{\boldsymbol{x}}(t_k) \\ \boldsymbol{\lambda}(t_k) \end{bmatrix} = \begin{bmatrix} \bar{Q}^{-1}(t_k)(Q(t_k)\bar{\boldsymbol{x}}(t_k) - \bar{R}\boldsymbol{\lambda}^*(t_k)) \\ \boldsymbol{\lambda}^*(t_k) \end{bmatrix} \tag{32}$$

  where $\mu > 0$. The solution $\boldsymbol{\lambda}^*(t_k)$ is obtained by solving $f_l(\boldsymbol{\lambda}, t_k) = 0$, $l \in \{1, 2, \ldots, 2n+1\}$ using an iterative generalized Newton's method, where each f_l is given by

$$f_l(\boldsymbol{\lambda}, t_k) = \bar{\boldsymbol{x}}' Q \bar{Q}^{-1} S_l \bar{Q}^{-1} Q \bar{\boldsymbol{x}} + \boldsymbol{\lambda}' \bar{R}' \bar{Q}^{-1} S_l \bar{Q}^{-1} \bar{R}\boldsymbol{\lambda} - 2\left(\bar{\boldsymbol{x}}' Q \bar{Q}^{-1} S_l + \boldsymbol{r}_l'\right) \bar{Q}^{-1} \bar{R}\boldsymbol{\lambda} + 2\boldsymbol{r}_l' \bar{Q}^{-1} Q \bar{\boldsymbol{x}}.$$

C. Intersample Output Predictor

In (24) and (25), we assumed that the observation $\boldsymbol{y}(t)$ is piecewise continuous in time, which is not (it is a discrete signal). A straightforward approach to deal with this problem is to hold $\boldsymbol{y}$ between sampling times. This, however, is not the best solution because it can introduce significant model mismatch if the interarrival times $t_{k+1} - t_k$ are not small enough. To overcome this problem, we suggest the use of an IOP such as the one described in [31]. For a general nonlinear system

$$\dot{\boldsymbol{x}}(t) = \boldsymbol{f}(\boldsymbol{x}(t), \boldsymbol{u}(t)), \quad \boldsymbol{y}(t_k) = \boldsymbol{h}(\boldsymbol{x}(t_k), \boldsymbol{u}(t_k))$$

the key idea consists of using the predicted output given by

$$\dot{\hat{\boldsymbol{y}}}(t) = \nabla_{\hat{\boldsymbol{x}}} \boldsymbol{h}(\hat{\boldsymbol{x}}, \boldsymbol{u}(t)) \boldsymbol{f}(\hat{\boldsymbol{x}}(t), \boldsymbol{u}(t)), \quad \hat{\boldsymbol{y}}(t_k) = \boldsymbol{y}(t_k)$$

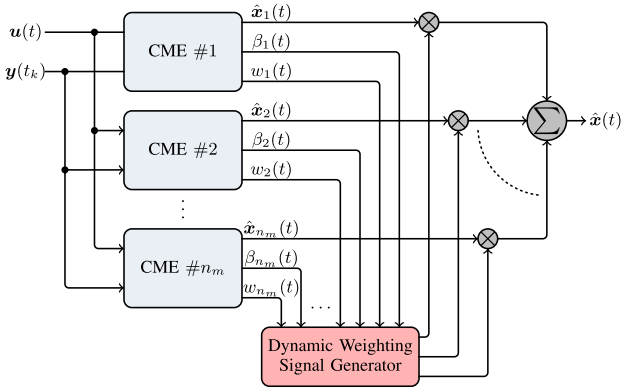

Fig. 3. Block diagram of the MMAE.

for $t \in [t_{k-1}, t_k)$. In our case, this corresponds to replacing the signals r_i in $A_{\boldsymbol{u},\boldsymbol{y}}$ (10) by $\hat{r}_i$, where

$$\dot{\hat{r}}_i(t) = -\left(\boldsymbol{v}'\left({}^{\mathcal{B}}\boldsymbol{p}_i + {}^{\mathcal{B}}\boldsymbol{q}_0\right) + \chi_c + \chi_{c_i}\right)\Big/\hat{r}_i, \quad t \in [t_{k-1}, t_k)$$
$$\hat{r}_i(t_k) = r_i(t_k).$$

D. Multiple Models

As discussed earlier, the process model (10) together with constraints (11)–(13) may not be observable, but only weakly observable (Theorem 1). In this case, the proposed CME converges to one of the two elements of $\mathcal{I}_r(\boldsymbol{x}_0)$ (18), (21), depending on the initial condition $\bar{\boldsymbol{x}}(0)$ of the observer. However, as soon as the system becomes observable, the state estimate will, as shown in the next section, converge to the true solution. In spite of this, there is still a problem of performance because the time that the estimate $\hat{\boldsymbol{x}}$ takes to reach a small neighborhood of the true solution $\boldsymbol{x}$ depends on the magnitude of the initial state error $\|\hat{\boldsymbol{x}}(0) - \boldsymbol{x}(0)\|$. This motivates the use of a multiple-model adaptive estimator (MMAE) [32] with the structure shown in Fig. 3. The MMAE consists of i) a bank of n_m local CME observers, where each observer is initialized with a different initial condition selected according to a suitable criterion (explained later) and ii) a dynamic weighting signal generator system that is responsible for updating the piecewise constant weights $p_s(t) \in [0, 1]$, $s = 1, 2, \ldots, n_m$. The (final) state estimate $\hat{\boldsymbol{x}}(t)$ is given by a weighted sum of the local state estimates, that is,

$$\hat{\boldsymbol{x}}(t) = \sum_{s=1}^{n_m} p_s(t_k)\hat{\boldsymbol{x}}_s(t), \quad t \in [t_k, t_{k+1})$$

where each $\hat{\boldsymbol{x}}_s(t)$, $s = 1, 2, \ldots n_m$, corresponds to a local state estimate generated by the sth local CME observer. Following the approach in [32] but adapted to the problem of continuous dynamics with discrete measurements, the weights are piecewise constant signals that are updated at measurements times $t = t_k$ according to:

$$p_s(t_k) = \frac{p_s(t_{k-1})\beta_s(t_k)e^{-w_s(t_k)}}{\sum_{l=1}^{n_m} p_l(t_{k-1})\beta_l(t_k)e^{-w_l(t_k)}}, \quad s \in \{1, 2, \ldots, n_m\}$$

where $\beta_s(\cdot)$ is a positive bounded signal and $w_s(\cdot)$ is an error measuring function that maps the observations of the system and the states of the sth local observer to a nonnegative real value. Examples of $\beta_s(\cdot)$ and $w_s(\cdot)$ are

$$\beta_s(t_k) = |\mathrm{S}_s(t_k)|^{-\frac{1}{2}}, \quad w_s(t_k) = \frac{1}{2}\|\hat{\boldsymbol{y}}_s(t_k^-) - \boldsymbol{y}(t_k)\|^2_{\mathrm{S}_s(t_k)^{-1}}$$
$$\mathrm{S}_s(t_k) = C_{\boldsymbol{u}}(t_k)Q^{-1}(t_k)C'_{\boldsymbol{u}}(t_k) + R_{\boldsymbol{n}} \succ 0.$$

In practice, to reduce memory and computing power, we have slightly modified the MMAE scheme according to the following procedure. Given the first range measurement obtained from a newly observed beacon i at time t_k, we generate two initial conditions for ${}^{\mathcal{B}}\bar{\boldsymbol{p}}_i(t_k)$ that satisfy constraints (11)–(13), using (21) and an arbitrarily chosen ${}^{\mathcal{B}}\bar{\boldsymbol{p}}_i(t_k)$ [which is typically set to $[0, r_i(t_k), 0]' + {}^{\mathcal{B}}\bar{\boldsymbol{q}}_0(t_k)$]. Two new CME observers are then created with the corresponding initial condition. Then, we apply an MMAE scheme with the weights initialized with $p_1(t_k) = p_2(t_k) = 0.5$ (for the case of two models). Whenever one of the weights $p_s(\cdot)$ reaches some threshold near one, the corresponding CME will be kept and all the other CMEs are discarded.

V. Observer Convergence

In this section, we investigate under what conditions the estimation error of the proposed observer converges to a small neighborhood of zero (or zero, in the absence of the measurement noise and process disturbances). We first analyze the stability properties of each local CME observer.

A. Convergence of the CME Observer

In what follows, we assume the following.

Assumption 1: The matrix $\bar{Q}(t)$ defined in (30) is positive definite along the trajectories of the CME, and $\bar{S}(\hat{\boldsymbol{x}}) + \bar{R}$ remains full column rank.

Assumption 2: Let $\mathtt{Num}(t, \sigma)$, $0 \le \sigma < t$, denote the number of time instants at which measurement arrives in the open interval (σ, t). There exist finite positive constants τ_D and N_0, for which the following condition holds:

$$\mathtt{Num}(t, \sigma) \le N_0 + (t - \sigma)/\tau_D. \tag{33}$$

Regarding the first assumption, note that Q is always positive definite, which means that $\bar{Q} \succ 0$ for the Lagrange multiplier $\boldsymbol{\lambda}$ sufficiently small. Also, the rank condition on $\bar{S}(\hat{\boldsymbol{x}}) + \bar{R}$ is the standard condition on Lagrange multiplier theory for constraint independence, which in this case holds because each constraint is imposed on a different beacon. Assumption 2 typically arises in the context of logic-based switching control and also in estimation of continuous systems with discrete observations [18]. The constant τ_D is called the average dwell time and N_0 the chatter bound. The condition above guarantees that the summation of $\|\boldsymbol{n}(\cdot)\|^2$ in (23) will not grow unbounded due to too frequent measurements. This assumption is purely technical and in practice always holds.

The next result establishes the convergence properties of the proposed CME observer. We will need the standard definition of class $\mathcal{K}$ and $\mathcal{KL}$ functions [33, p. 144].

Theorem 6: Suppose that Assumptions 1 and 2 hold and denote $\boldsymbol{e}_1 := \bar{\boldsymbol{x}} - \boldsymbol{x}$. Let $\boldsymbol{u}(t)$, $\boldsymbol{y}(t_k)$ be a given input/output pair for system (22). Then, there exist a $\mathcal{KL}$ function β, and class $\mathcal{K}$ functions γ_d and γ_n such that the estimation error associated with the CME observer satisfies

$$\|\bar{\boldsymbol{e}}(t)\| \le \beta(\|\boldsymbol{e}(0)\|, t) + \gamma_d\Big(\sup_{\tau\in[0,t]} \|\boldsymbol{d}(\tau)\|_{R_d^{-1}}\Big) + \gamma_n\Big(\sup_{t_\tau\in[0,t]} \|\boldsymbol{n}(t_\tau)\|_{R_n^{-1}}\Big) \tag{34}$$

where $\bar{\boldsymbol{e}} := [\boldsymbol{e}'_1, \boldsymbol{e}'_2, \boldsymbol{e}'_3]'$ and $\boldsymbol{e}_2$, $\boldsymbol{e}_3$ are defined in (29).

Proof: Consider the following Lyapunov functions:

$$V_1 = \boldsymbol{e}'_1 Q(t)\boldsymbol{e}_1, \quad V_2 = \boldsymbol{e}'_2\boldsymbol{e}_2/2 + \boldsymbol{e}'_3\boldsymbol{e}_3/2 \tag{35}$$

which are bounded below and above by some class $\mathcal{K}$ functions. Consider first the case where $t \in [t_{k-1}, t_k)$ for some sampling times t_{k-1} and t_k. Computing the time derivative of V_1 and V_2 yields

$$\begin{aligned}
\dot{V}_1 &= -\boldsymbol{e}'_1\big(QA_{\boldsymbol{u},\boldsymbol{y}} + A'_{\boldsymbol{u},\boldsymbol{y}}Q + QG_{\boldsymbol{u}}R_{\boldsymbol{d}}G'_{\boldsymbol{u}}Q\big)\boldsymbol{e}_1 \\
&\quad + \boldsymbol{e}'_1 Q(A_{\boldsymbol{u},\boldsymbol{y}}\boldsymbol{e}_1 - G_{\boldsymbol{u}}\boldsymbol{d}) + (A_{\boldsymbol{u},\boldsymbol{y}}\boldsymbol{e}_1 - G_{\boldsymbol{u}}\boldsymbol{d})'Q\boldsymbol{e}_1 \\
&= -\frac{1}{2}\big\|G'_{\boldsymbol{u}}Q\boldsymbol{e}_1\big\|^2_{R_{\boldsymbol{d}}} - \frac{1}{2}\big\|G'_{\boldsymbol{u}}Q\boldsymbol{e}_1 + 2R_{\boldsymbol{d}}^{-1}\boldsymbol{d}\big\|^2_{R_{\boldsymbol{d}}} + 2\|\boldsymbol{d}\|^2_{R_{\boldsymbol{d}}^{-1}} \\
\dot{V}_2 &= \boldsymbol{e}'_3(2(\bar{S}(\hat{\boldsymbol{x}}) + \bar{R})'\dot{\hat{\boldsymbol{x}}}) \\
&\quad + \boldsymbol{e}'_2(\dot{\bar{Q}}\dot{\hat{\boldsymbol{x}}} - Q\ddot{\hat{\boldsymbol{x}}} + \dot{Q}\dot{\hat{\boldsymbol{x}}} - \dot{Q}\dot{\bar{\boldsymbol{x}}} + (\dot{\bar{S}}(\hat{\boldsymbol{x}}) + \dot{\bar{R}})\boldsymbol{\lambda}) \\
&= \begin{bmatrix}\boldsymbol{e}_2\\ \boldsymbol{e}_3\end{bmatrix}\Bigg(\begin{bmatrix}\bar{Q} & \bar{S}(\hat{\boldsymbol{x}}) + \bar{R}\\ \bar{S}(\hat{\boldsymbol{x}})' + \bar{R}' & \boldsymbol{0}\end{bmatrix}\begin{bmatrix}\dot{\hat{\boldsymbol{x}}}\\ \dot{\boldsymbol{\lambda}}\end{bmatrix} \\
&\qquad + \begin{bmatrix}\dot{Q}\hat{\boldsymbol{x}} - Q\dot{\hat{\boldsymbol{x}}} - \dot{Q}\bar{\boldsymbol{x}}\\ \boldsymbol{0}\end{bmatrix}\Bigg).
\end{aligned}$$

Using Assumption 1, (31), and the fact that $\delta I \le G_{\boldsymbol{u}}R_{\boldsymbol{d}}G'_{\boldsymbol{u}} \le \Delta I$, we can conclude that

$$\dot{V}_1 \le -\frac{1}{2}\delta\lambda_{\min}(Q)V_1 + 2\|\boldsymbol{d}\|^2_{R_{\boldsymbol{d}}^{-1}}, \quad \dot{V}_2 = -2\mu V_2$$

where $\lambda_{\min}(Q)$ is the smallest eigenvalue of matrix Q. Note that observability of system (22) is a necessary and sufficient condition for $\lambda_{\min}(Q) > 0$. Defining $\gamma := (1/2)\delta \inf_{\tau\in[t_{k-1},t)} \lambda_{\min}(Q(\tau))$, we further conclude that

$$V_1(t) \le V_1(t_{k-1})e^{-\gamma(t-t_{k-1})} + \frac{2}{\gamma}\sup_{\tau\in[t_{k-1},t)} \|\boldsymbol{d}(\tau)\|^2_{R_{\boldsymbol{d}}^{-1}} \tag{36}$$

$$V_2(t) = V_2(t_{k-1})e^{-2\mu(t-t_{k-1})} \tag{37}$$

for $t \in [t_{k-1}, t_k)$. Note that from (37), it follows that the conditions in (29) will be enforced (for sufficiently large μ and/or t_k).

Now consider the case where $t = t_k$. Using (27), we obtain

$$\boldsymbol{e}_1(t_k) = (I - Q^{-1}(t_k)\Psi(t_k))\boldsymbol{e}_1(t_k^-) + Q^{-1}(t_k)\bar{\boldsymbol{n}}(t_k) \tag{38}$$

where $\bar{\boldsymbol{n}}(t_k) = C'_{\boldsymbol{u}}R_n^{-1}\boldsymbol{n}(t_k)$ and $\Psi(t_k) = C'_{\boldsymbol{u}}R_{\boldsymbol{n}}^{-1}C_{\boldsymbol{u}}$. Thus, substituting (38) into (35) and considering the composite function $V = V_1 + V_2$, we obtain

$$\begin{aligned}
V(t_k) &= \boldsymbol{e}_1(t_k^-)'(Q(t_k) + \Psi(t_k)Q^{-1}(t_k)\Psi(t_k) - 2\Psi(t_k))\boldsymbol{e}_1(t_k^-) \\
&\quad + 2\boldsymbol{e}_1(t_k^-)'(I - \Psi(t_k)Q^{-1}(t_k))\bar{\boldsymbol{n}}(t_k) \\
&\quad + \bar{\boldsymbol{n}}(t_k)'Q^{-1}(t_k)\bar{\boldsymbol{n}}(t_k) \\
&\quad + \frac{1}{2}\|\bar{Q}(t_k)\hat{\boldsymbol{x}}(t_k) - Q(t_k)\bar{\boldsymbol{x}}(t_k)\|^2 + \frac{1}{2}\|\bar{S}(\hat{\boldsymbol{x}})'\hat{\boldsymbol{x}}\|^2.
\end{aligned}$$

Note that using Assumption 1 and (32), it follows that $V_2(t_k) = 0$. Using the matrix inversion lemma [34] and (26), we can further simplify the terms in the above expression containing $Q(t_k)$ as

$$\begin{aligned} I - \Psi Q^{-1}(t_k) &= I - L'FLQ^{-1} \\ Q(t_k) + \Psi Q^{-1}(t_k)\Psi - 2\Psi &= Q - L'FL \\ Q^{-1}(t_k) &= Q^{-1} - Q^{-1}L'FLQ^{-1} \end{aligned}$$

where $Q = Q(t_k^-)$, $L = \Psi^{1/2}(t_k)$ is any matrix such that $L'L = \Psi(t_k)$, and $F = (I + LQ^{-1}L')^{-1}$ is a positive definite matrix. This leads to

$$\begin{aligned} V(t_k) &= V_1(t_k^-) - \boldsymbol{e}_1(t_k^-)'(L'FL)\boldsymbol{e}_1(t_k^-) \\ &\quad + 2\boldsymbol{e}_1(t_k^-)'(I - L'FLQ^{-1})\bar{\boldsymbol{n}}(t_k) \\ &\quad + \bar{\boldsymbol{n}}(t_k)'(Q^{-1} - Q^{-1}L'FLQ^{-1})\bar{\boldsymbol{n}}(t_k) \\ &\le V(t_k^-) + \bar{\boldsymbol{n}}(t_k)'Q^{-1}\bar{\boldsymbol{n}}(t_k) + 2\boldsymbol{e}_1(t_k^-)'\bar{\boldsymbol{n}}(t_k) \\ &\quad - \left\| F^{\frac{1}{2}}L\boldsymbol{e}_1(t_k^-) - F^{\frac{1}{2}}LQ^{-1}\bar{\boldsymbol{n}}(t_k) \right\|^2 \\ &\le (1+\epsilon)V(t_k^-) + (1 + 1/\epsilon)\bar{\boldsymbol{n}}(t_k)'Q^{-1}\bar{\boldsymbol{n}}(t_k) \end{aligned} \tag{39}$$

where ϵ is an arbitrary small positive constant. Now, by combining (39) with (36) and (37), it follows that:

$$\begin{aligned} V(t_k) \le (1+\epsilon)\big[V_1(t_{k-1})e^{-\gamma\,\Delta t_k} + V_2(t_{k-1})e^{-2\mu\,\Delta t_k}\big] \\ + (\epsilon+1)a_k/\epsilon + b_k \end{aligned} \tag{40}$$

where $\Delta t_k = t_k - t_{k-1}$, $a_k = \lambda_{\max}(Q^{-1})\|\bar{\boldsymbol{n}}(t_k)\|^2$, and $b_k = (2(1+\epsilon)/\gamma)\sup_{\tau\in[t_{k-1},t_k)}\|\boldsymbol{d}(\tau)\|^2_{R_{\boldsymbol{d}}^{-1}}$. Solving (40) recursively yields

$$\begin{aligned} V(t_k) \le (1+\epsilon)^k\big[V_1(t_0)e^{\gamma(t_0-t_k)} + V_2(t_0)e^{2\mu(t_0-t_k)}\big] \\ + \sum_{j=0}^{k-1}(1+\epsilon)^j e^{\gamma(t_{k-j}-t_k)}((\epsilon+1)a_{k-j}/\epsilon + b_{k-j}). \end{aligned}$$

Using Assumption 2 and (33), we can further simplify the above inequality to

$$\begin{aligned} V(t_k) \le [(1+\epsilon)e^{-\gamma\tau_D}]^k e^{\gamma N_0\tau_D}V_1(t_0) \\ + [(1+\epsilon)e^{-2\mu\tau_D}]^k e^{2\mu N_0\tau_D}V_2(t_0) \\ + \sum_{j=0}^{k-1}[(1+\epsilon)e^{-\gamma\tau_D}]^j((\epsilon+1)a_{k-j}/\epsilon + b_{k-j})e^{\gamma N_0\tau_D}. \end{aligned}$$

By choosing μ and ϵ such that $\kappa_1 := (1+\epsilon)e^{-\gamma\tau_D} < 1$ and $\kappa_2 := (1+\epsilon)e^{-2\mu\tau_D} < 1$, it follows that V is a bounded function and $V(t) \to (1/1-\kappa_1)((\epsilon+1/\epsilon)\max_k a_k + \max_k b_k)e^{\gamma\max_k\{N_0\tau_D\}}$ as $t\to\infty$. Using the fact that $\|\bar{\boldsymbol{e}}\| \le \|\boldsymbol{e}_1\| + \|\boldsymbol{e}_2\| + \|\boldsymbol{e}_3\|$, we can now conclude inequality (34). □

In Theorem 6, we have used the fact that Q is a positive definite matrix that is bounded below, which means that $\lambda_{\min}(Q) > 0$. This is true if the system is observable, that is, the observability matrix is full rank. This can be done either using range and depth measurements or, in the case of range only measurements, using at least two noncollinear piecewise constant angular velocities. Note also that the estimate $\hat{\boldsymbol{x}}(t)$ is the solution to the optimization problem (28) pointwise at times t_k and converges asymptotically to the optimal in the intervals $[t_{k-1}, t_k)$.

Remark 1: Consider system (10) without disturbance $\boldsymbol{d}(\cdot)$ and noise $\boldsymbol{n}(\cdot)$. In this case, it can be concluded that as $t\to\infty$, the functions $V_1(t)$ and $V_2(t)\to 0$, which implies that $\bar{\boldsymbol{x}}(t)\to\boldsymbol{x}(t)$, $(\bar{S}(\hat{\boldsymbol{x}}(t)) + 2\bar{R})'\hat{\boldsymbol{x}}(t)\to 0$, from which it follows that $(\hat{\boldsymbol{x}}-\bar{\boldsymbol{x}})'Q(\hat{\boldsymbol{x}}-\bar{\boldsymbol{x}})\to 0$. Since $Q\succ 0$, it follows that $\hat{\boldsymbol{x}}(t)\to\bar{\boldsymbol{x}}(t)$, and therefore $\hat{\boldsymbol{x}}(t)\to\boldsymbol{x}(t)$ as $t\to\infty$.

B. Convergence of the MMAE

So far, we have investigated the convergence properties of each local CME observer, which implies that Theorem 6 and Remark 1 apply to each CME in the multiple-model approach. We now show that similar properties apply to the state estimate computed using the MMAE architecture. The next result provides conditions for the convergence of the dynamic weights $p_s(t)$. Roughly speaking, it says that the model identified is the one that exhibits least output error (residual) energy. The proof is omitted because it would be a slightly variation of the one in [32].

Lemma 1: Let $s^\star \in \{1,\dots,n_m\}$ be an index corresponding to one of the CME observers, and let $\mathcal{S} = \{1,\dots,n_m\}\setminus\{s^\star\}$ be an index set. Suppose that there exist positive constants n' and k' such that for all $k\ge k'$ and $n\ge n'$, the following condition holds for all $j\in\mathcal{S}$:

$$\sum_{\tau=k}^{k+n-1}(w_{s^\star}(t_\tau) - \ln\beta_{s^\star}(t_\tau)) < \sum_{\tau=k}^{k+n-1}(w_j(t_\tau) - \ln\beta_j(t_\tau)). \tag{41}$$

Then $p_{s^\star}(t)\to 1$ as $t\to\infty$.

Condition (41) can be viewed as a distinguishability criterion. The following result establishes the convergence of the proposed observer.

Theorem 7: Suppose that Assumptions 1 and 2 hold, and let $\boldsymbol{u}(t)$, $\boldsymbol{y}(t_k)$ be a given input/output pair of system (22). Then, there exist a $\mathcal{KL}$ function β, and class $\mathcal{K}$ functions γ_d and γ_n such that the estimation error associated with the MMAE is bounded and satisfies

$$\begin{aligned} \|\boldsymbol{e}_M(t)\| \le \beta(\|\boldsymbol{e}_M(0)\|, t) + \gamma_d\Big(\sup_{\tau\in[0,t]}\|\boldsymbol{d}(\tau)\|_{R_{\boldsymbol{d}}^{-1}}\Big) \\ + \gamma_n\Big(\sup_{t_\tau\in[0,t]}\|\boldsymbol{n}(t_\tau)\|_{R_{\boldsymbol{n}}^{-1}}\Big) \end{aligned} \tag{42}$$

where $\boldsymbol{e}_M(t)$ is the weighted sum of the error vectors associated with each model defined in Theorem 6, that is

$$\boldsymbol{e}_M(t) := \sum_{s=1}^{n_m} p_s(t)\bar{\boldsymbol{e}}_s(t). \tag{43}$$

Suppose also that the distinguishability criterion (41) holds. Then, there exists an index $s^*\in\{1,2,\dots,n_m\}$ such that $\boldsymbol{e}_M(t)\to\bar{\boldsymbol{e}}_{s^*}(t)$ as $t\to\infty$.

Proof: From (34) and (43), we can conclude that

$$\begin{aligned} \|\boldsymbol{e}_M(t)\| \le \sum_{s=1}^{n_m} p_s(t)\Big(\beta_s(\|\bar{\boldsymbol{e}}_s(0)\|, t) + \gamma_{d_s}\Big(\sup_{\tau\in[0,t]}\|\boldsymbol{d}(\tau)\|_{R_{\boldsymbol{d}}^{-1}}\Big) \\ + \gamma_{n_s}\Big(\sup_{t_\tau\in[0,t]}\|\boldsymbol{n}(t_\tau)\|_{R_{\boldsymbol{n}}^{-1}}\Big)\Big) \end{aligned}$$

for some $\beta_s\in\mathcal{KL}$ and $\gamma_{d_s},\gamma_{n_s}\in\mathcal{K}$, $s\in\{1,2,\dots,n_m\}$. Thus, there exist class $\mathcal{KL}$ function β and class $\mathcal{K}$ functions

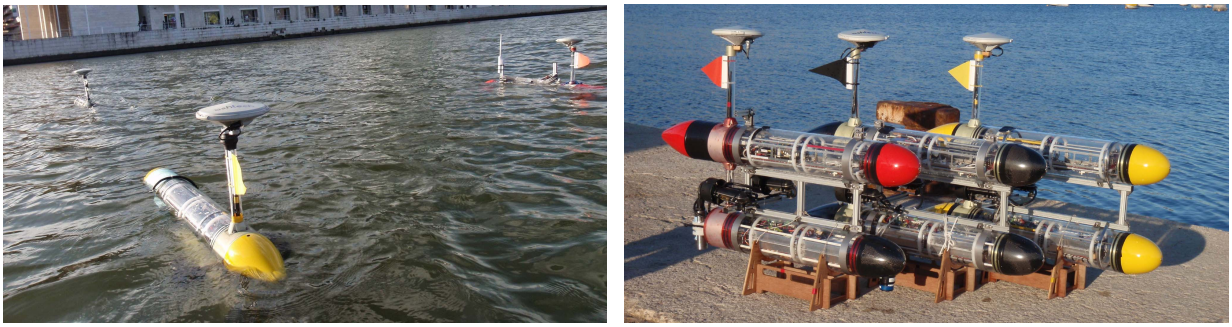

Fig. 4. Three MEDUSA marine robotic vehicles.

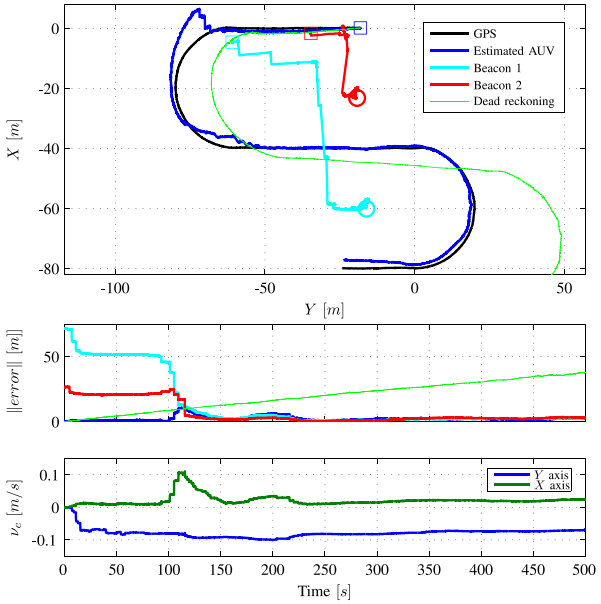

Fig. 5. Mission 1. Top: trajectory of the AUV (GPS, estimated using DR only, and estimated using the proposed observer) and beacon locations (true position denoted by O and estimated with the initial condition □). Bottom: estimation errors and estimated current velocity.

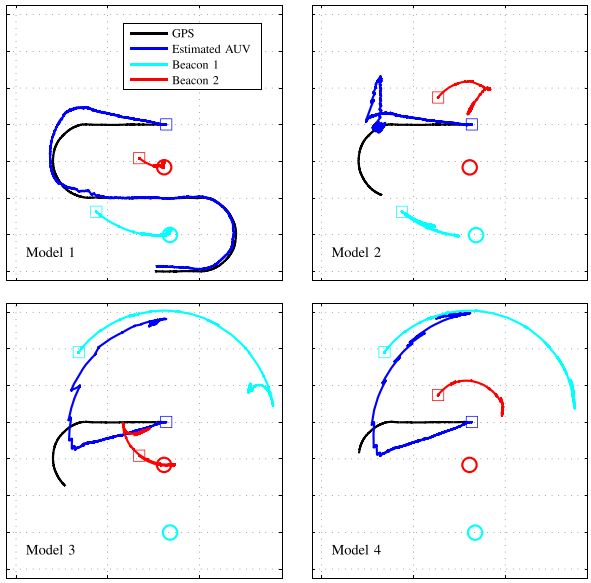

Fig. 6. Evolution of the AUV and estimated beacon positions for each model presented in the xy plane, corresponding to mission 1.

γ_d and γ_n such that (42) holds. Now, if the distinguishability criterion (41) holds, we can conclude that $p_{s^*} \to 1$ and $p_s \to 0, \forall s \in \mathcal{S}$. This implies that $\boldsymbol{e}_M(t) \to \bar{\boldsymbol{e}}_{s^*}(t)$ as $t \to \infty$. □

VI. EXPERIMENTAL RESULTS

In this section, we describe a set of experiments carried out with three autonomous marine vehicles of the MEDUSA class (Fig. 4). Each vehicle has two side thrusters that can be independently controlled to impart forward and rotational motion and is equipped with an attitude and heading reference unit that provides measurement of body orientation $\boldsymbol{\eta}(t)$ and angular velocity $\boldsymbol{\omega}(t)$. To measure the forward velocity $\nu(t)$, and since this class of vehicles do not carry a Doppler velocity logger, an online computational procedure was used to estimate it based on the readings of the commands that are sent to the thrusters and using a quasi-steady-state model of the vehicle [35]. A GPS unit was used for ground-truth comparison purposes. Each vehicle is equipped with an acoustic Tritech Micron data modem and ranging unit that is used for communications and also to measure the ranges among vehicles. The tests were performed in open water, in June 2012 in the Expo area of Lisbon, Portugal (latitude: 38.766 and longitude: −9.03) [Fig. 4 (left)]. See [17] and [35] for more information on MEDUSA autonomous marine vehicles and the experimental site in Lisbon. Throughout the tests, two of the MEDUSA vehicles were kept in a hold position mode to act as proxies for stationary beacons. The other MEDUSA maneuvered at the surface and acted as proxy for an underwater vehicle moving at a constant depth, interrogating the beacons. This is realistic, because the vehicle does not use GPS or aerial communications for localization purposes.

Due to space limitations, only three types of trajectories for the moving MEDUSA are described.

1) A lawn-mower trajectory (Fig. 5) where the observability conditions are not satisfied initially. However, as soon as the AUV turns, the observability condition (17) holds.
2) A small circular trajectory performed with (commanded) angular velocity $\omega_{e_z} = 0.025$ rad/s (Fig. 7). The observability condition is satisfied from the time the AUV starts.
3) A larger circumference performed with (commanded) angular velocity $\omega_{e_z} = 0.012$ rad/s (Fig. 8). Since the angular velocity ω_{e_z} is smaller, when compared with the second mission, different results are expected.

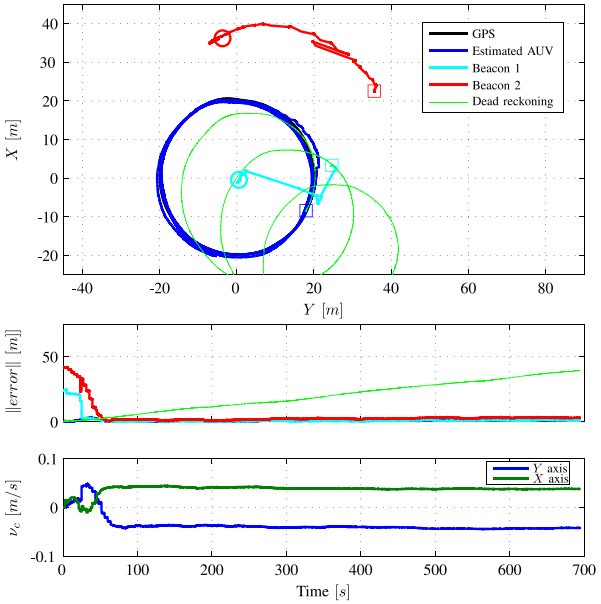

Fig. 7. Mission 2. Top: trajectory of the AUV (GPS, estimated using DR only, and estimated using the proposed observer) and beacon locations (true position denoted by O and estimated with the initial condition □). Bottom: estimation errors and estimated current velocity.

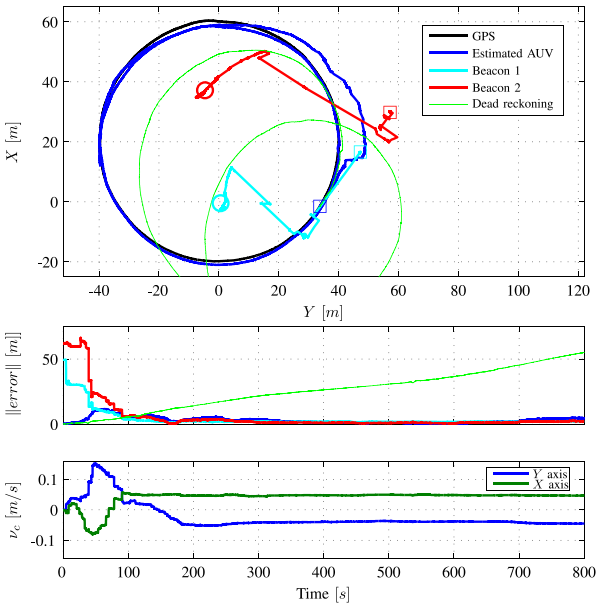

Fig. 8. Mission 3. Top: trajectory of the AUV (GPS, estimated using DR only, and estimated using the proposed observer) and beacon locations (true position denoted by O and estimated with the initial condition □). Bottom: estimation errors and estimated current velocity.

The moving MEDUSA, which starts at the initial position identified by the symbol (□), moves with a commanded forward velocity of 0.5 m/s and interrogates each beacon in cycles of 4 s, which guarantees that the interarrival time condition (45) holds. After extensive trials, we concluded that the range measurements acquired by the modems can be modeled as being corrupted with additive noise with a bounded error of 0.3 m. In these experiments, it was observed that the movement of the AUV was affected by constant ocean currents. Thus, without the knowledge of the ocean current vector, the DR error accumulates very fast (see the DR error in Figs. 5–8).

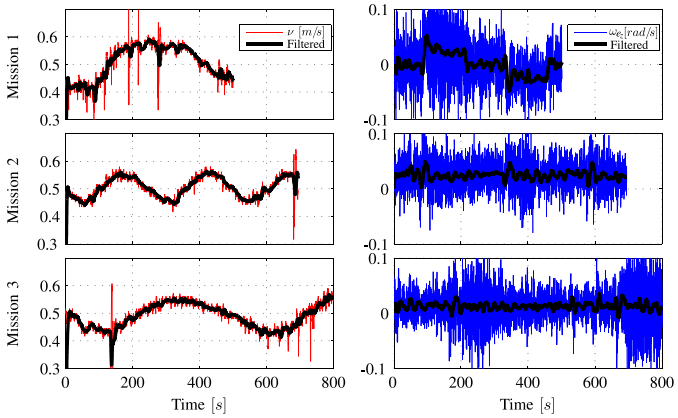

Fig. 9. Linear and angular velocities of the AUV for missions 1–3. Filtered data are shown with a black solid line.

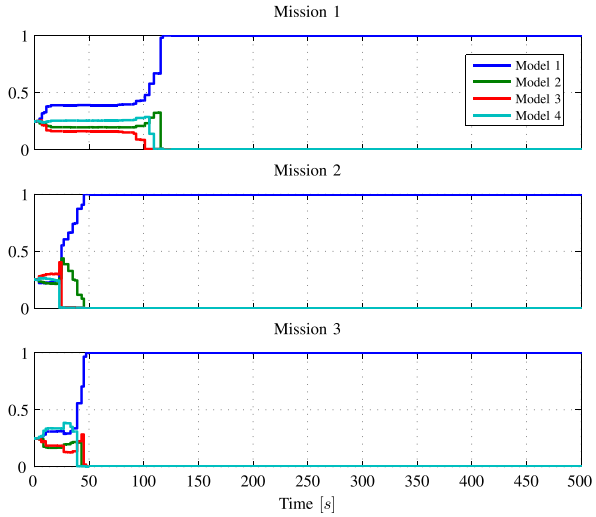

Fig. 10. Time evolution of the models' weights for missions 1–3.

The local estimators in the proposed multiple-model observer approach are initialized, as described in Section IV, meaning that one of the initial estimates of the position of each beacon is on the left-hand side of the AUV and the other one on the right. The design parameters for the observers were set to $Q(0) = \text{diag}([10^2 I_2, 10^{-2} I_4, 10^2 I_2, 0.1 I_3, 10 I_2])$, $R_n = 0.25 I_2$, $R_d = \text{diag}([5 \times 10^{-3} I_2, 10^{-6} I_6, 0.1 I_3, 10^{-6}, 10^{-4} I_2])$, and $\mu = 10$ in the appropriate units.

1) Mission 1: Fig. 5 shows the trajectory of the AUV (GPS, estimated trajectory using DR only, and estimated trajectory using the proposed observer), the beacon locations (the true locations and their estimates), estimation errors, and estimated current velocity for mission 1. Clearly, as soon as the vehicle turns and therefore the system becomes observable, the estimation error of the observer initialized with the arbitrary chosen initial condition converges to a small value close to zero. This can also be observed in the evolution of the estimated state of each local estimator, as shown in Fig. 6. In this case, model 1 converges to the true locations of the beacons, while the other models converge to some or all of the mirror points for each beacon. The evolution of the models' weights is shown in Fig. 10, where the weight of model 1 converges to one since it has the least error function.

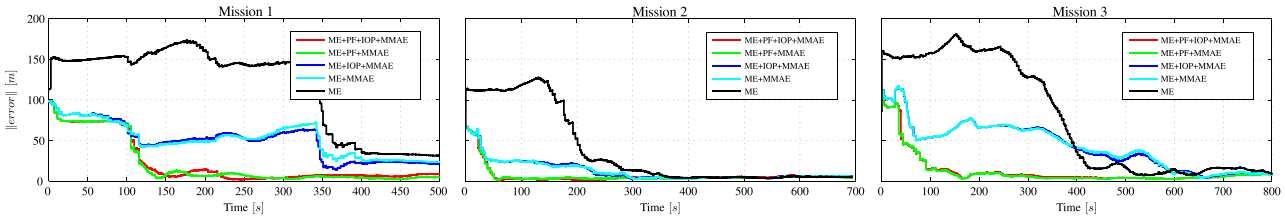

Fig. 11. Comparison of different observers for missions 1–3.

2) Mission 2: In this mission (Fig. 7), $\omega_{e_z} > 0$ (see Fig. 9), and therefore the observability condition (17) holds. Thus, convergence of the estimator is achieved much faster when compared with the first mission. This can also be observed from the convergence of the models' weights shown in Fig. 10.

3) Mission 3: In the last mission, the AUV moves on a larger circumference (Fig. 8), with an average angular velocity that is half of that in the second mission (Fig. 9). Although convergence of the models' weights is similar to that observed in mission 2 (Fig. 10), the same is not true for the convergence of the states errors, which is slower. This is due to the smaller magnitude of the angular velocity ω_{e_z}, which leads to an observability matrix with a higher condition number and a smaller minimum singular value. These two values are a measure of the quality of the unobservability of the system and the corresponding estimator. The reader is referred to [36] and [37] for a discussion of these unobservability measures.

In Fig. 11, we compare the effect of disabling one or more of the designed blocks in the three missions. We consider five observers:

1) complete observer consisting of the ME, PF, IOP, and MMAE blocks;
2) observer without the IOP module;
3) observer without using the PF module, which solves the unconstrained problem;
4) observer with only the ME and MMAE modules;
5) plain ME observer.

As expected, taking into account the quadratic constraint together with the IOP and the MMAE along with the ME observer significantly improves the convergence of the estimation error during the transient phase, when compared with the unconstrained ME observer. Note also in missions 2 and 3 that after sufficient time has elapsed, there is no significant difference in the performance of these observers. This shows that the output of the PF, $\hat{\boldsymbol{x}}$, converges to the output of ME, $\bar{\boldsymbol{x}}$, meaning that $\bar{\boldsymbol{x}}$ satisfies constraints (11)–(13).

VII. Conclusion

This paper addressed theoretical and practical issues related to the problem of range-based simultaneous AUV/multibeacon localization in the presence of ocean currents. Conditions were derived under which it is possible to reconstruct the initial condition of the system under study. The latter includes the position of the beacons and the vehicle. In the model adopted for localization system design, the states evolve continuously with time, but the range measurements are only available at discrete instants of time, in a possible nonuniform manner. Motivated by practical considerations that have to do with maneuverability and energy-related issues, we considered the important case where the AUV undergoes motion along trimming trajectories. We have shown that this class of trajectories, which are sufficiently general to be of practical use, allow for a simple characterization of the types of maneuvers that yield observability or weak observability of the underlying design model. In particular, we proved that generically, for an arbitrary range measurement schedule, if either the position of one of the beacons or the initial position of the AUV is known, then there are trimming trajectories such that even without depth information, the model is weakly observable. In the process of deriving these results, we obtained a complete mathematical characterization of the unobservable space and interpreted it geometrically. If depth measurements are also available, then the mode is observable even in the presence of unknown constant ocean currents. The results derived have a strong practical implication in that the concatenation of at least two appropriately chosen different trimming trajectories that do not necessarily yield observability individually leads to an observable system.

Equipped with these results, in the second part of this paper, we proposed a novel multiple-model observer for simultaneous AUV and beacon localization. The setup adopted was motivated by the fact that some of the trajectories used may yield temporary unobservability over a finite interval of time, thus warranting the use of multiple models running in parallel. The resulting observer borrows concepts from ME estimation theory, PFs, and multiple-model estimation techniques. Convergence analysis of the resulting observer system was formally done. The results of field experiments with a robotic marine vehicle showed the efficacy of the simultaneous AUV/multiple beacon localization system.

Appendix

The following proposition is instrumental in analyzing the impact of the sampling times on the observability properties of systems (14) and (16).

Proposition 1: Consider $w > 0$, and let $t_1 < t_2 < \cdots < t_n$, $n \geq 7$ be consecutive sampling times. Then the matrix $\mathcal{O}_{\boldsymbol{t}} \in \mathbb{R}^{n\times 7}$ composed by rows of the form

$$\mathcal{O}_{t_i} = \begin{bmatrix} 1 & t_i & t_i^2 & \sin(t_i w) & \cos(t_i w) & t_i \sin(t_i w) & t_i \cos(t_i w) \end{bmatrix}$$

is full column rank, except on a zero measure set given by $|\bar{\mathcal{O}}_{\boldsymbol{t}}| = 0$ with

$$\bar{\mathcal{O}}_{\boldsymbol{t}} = \begin{bmatrix} A & B \\ C & D \end{bmatrix}, \quad A = \begin{bmatrix} \bar{\beta}_{42} - \bar{\beta}_{32} & \bar{\alpha}_{42} - \bar{\alpha}_{32} \\ \bar{\beta}_{52} - \bar{\beta}_{42} & \bar{\alpha}_{52} - \bar{\alpha}_{42} \end{bmatrix}$$

$$B = \begin{bmatrix} \bar{\beta}_{41} - \bar{\beta}_{31} & \bar{\alpha}_{41} - \bar{\alpha}_{31} \\ \bar{\beta}_{51} - \bar{\beta}_{41} & \bar{\alpha}_{51} - \bar{\alpha}_{41} \end{bmatrix}$$

$$C = \begin{bmatrix} \bar{\beta}_{62} - \bar{\beta}_{52} & \bar{\alpha}_{62} - \bar{\alpha}_{52} \\ \bar{\beta}_{72} - \bar{\beta}_{62} & \bar{\alpha}_{72} - \bar{\alpha}_{62} \end{bmatrix}$$

$$D = \begin{bmatrix} \bar{\beta}_{61} - \bar{\beta}_{51} & \bar{\alpha}_{61} - \bar{\alpha}_{51} \\ \bar{\beta}_{71} - \bar{\beta}_{61} & \bar{\alpha}_{71} - \bar{\alpha}_{61} \end{bmatrix}$$

and $\bar{\beta}_{ij} = (\sin(t_i w) - \sin(t_j w)/t_i - t_j)$ and $\bar{\alpha}_{ij} = (\cos(t_i w) - \cos(t_j w)/t_i - t_j)$. In particular, suppose that the interarrival times are uniform, that is, $t_{k+1} - t_k = T$ for all $t_k \in [t_0, t_f)$. Then, the matrix $\mathcal{O}_t$ is full column rank except on a zero measure set described by (19).

Proof: Consider the following matrices P_1, P_2, P_3, P_4, and P_5 defined as:

$$P_1 := I_7 - \begin{bmatrix} \mathbf{0} & t_1 I_2 & s_1 & c_1 & \mathbf{0} \\ 0 & \mathbf{0} & 0 & 0 & \mathbf{0} \\ \mathbf{0} & \mathbf{0} & \mathbf{0} & \mathbf{0} & t_1 I_2 \\ \mathbf{0} & \mathbf{0} & \mathbf{0} & \mathbf{0} & \mathbf{0} \end{bmatrix}$$

$$P_2 := I_6 - \begin{bmatrix} 0 & t_2 & \bar{\beta}_{21} & \bar{\alpha}_{21} & s_2 & c_2 \\ \mathbf{0} & \mathbf{0} & \mathbf{0} & \mathbf{0} & \mathbf{0} & \mathbf{0} \end{bmatrix}$$

$$P_3 := I_5 - \begin{bmatrix} 0 & \bar{\gamma}_{32} & \bar{\nu}_{32} & \bar{\beta}_{32} & \bar{\alpha}_{32} \\ \mathbf{0} & \mathbf{0} & \mathbf{0} & \mathbf{0} & \mathbf{0} \end{bmatrix},$$

$$P_4 := I_4 - \begin{bmatrix} \mathbf{0} & 0 \\ I_3 & \mathbf{0} \end{bmatrix}, P_5 := \begin{bmatrix} \mathbf{0} & (t_1 - t_2) I_2 \\ I_2 & I_2 \end{bmatrix}$$

where $s_i = \sin(t_i w)$, $c_i = \cos(t_i w)$, $\bar{\gamma}_{j2} = ((\bar{\beta}_{j1} - \bar{\beta}_{21})/(t_j - t_2))$, and $\bar{\nu}_{j2} = ((\bar{\alpha}_{j1} - \bar{\alpha}_{21})/(t_j - t_2))$, $i \in \{1, \ldots, 7\}$, $j \in \{3, \ldots, 7\}$.

Note that the determinant of the above matrices with exception of P_5 is one, that is, $|P_5| = (t_2 - t_1)^2 > 0$. Thus, we may conclude that the determinant of $\mathcal{O}_{\boldsymbol{t}}$, composed by the first seven row vectors $\mathcal{O}_{t_i}, i \in \{1, 2, \ldots, 7\}$, satisfies

$$\begin{aligned} |\mathcal{O}_{\boldsymbol{t}}| &= |\mathcal{O}_{\boldsymbol{t}} \cdot P_1| \\ &= \prod_{i=2}^{7} (t_i - t_1) \left| \begin{bmatrix} 1 & t_2 & \bar{\beta}_{21} & \bar{\alpha}_{21} & s_2 & c_2 \\ \vdots & \vdots & \vdots & \vdots & \vdots & \vdots \\ 1 & t_7 & \bar{\beta}_{71} & \bar{\alpha}_{71} & s_7 & c_7 \end{bmatrix} \cdot P_2 \right| \\ &= \prod_{i=2}^{7} (t_i - t_1) \prod_{i=3}^{7} (t_i - t_2) \left| \begin{bmatrix} 1 & \bar{\gamma}_{32} & \bar{\nu}_{32} & \bar{\beta}_{32} & \bar{\alpha}_{32} \\ \vdots & \vdots & \vdots & \vdots & \vdots \\ 1 & \bar{\gamma}_{72} & \bar{\nu}_{72} & \bar{\beta}_{72} & \bar{\alpha}_{72} \end{bmatrix} \cdot P_3 \right| \\ &= (t_2 - t_1)^{-2} \prod_{i=2}^{7} (t_i - t_1) \prod_{i=3}^{7} (t_i - t_2) \\ &\quad \left| P_4 \cdot \begin{bmatrix} \bar{\gamma}_{42} - \bar{\gamma}_{32} & \bar{\nu}_{42} - \bar{\nu}_{32} & \bar{\beta}_{42} - \bar{\beta}_{32} & \bar{\alpha}_{42} - \bar{\alpha}_{32} \\ \bar{\gamma}_{52} - \bar{\gamma}_{32} & \bar{\nu}_{52} - \bar{\nu}_{32} & \bar{\beta}_{52} - \bar{\beta}_{32} & \bar{\alpha}_{52} - \bar{\alpha}_{32} \\ \bar{\gamma}_{62} - \bar{\gamma}_{32} & \bar{\nu}_{62} - \bar{\nu}_{32} & \bar{\beta}_{62} - \bar{\beta}_{32} & \bar{\alpha}_{62} - \bar{\alpha}_{32} \\ \bar{\gamma}_{72} - \bar{\gamma}_{32} & \bar{\nu}_{72} - \bar{\nu}_{32} & \bar{\beta}_{72} - \bar{\beta}_{32} & \bar{\alpha}_{72} - \bar{\alpha}_{32} \end{bmatrix} \cdot P_5 \right| \\ &= (t_2 - t_1)^{-2} \prod_{i=2}^{7} (t_i - t_1) \prod_{i=3}^{7} (t_i - t_2) |\bar{\mathcal{O}}_{\boldsymbol{t}}|. \end{aligned} \tag{44}$$

Since $t_i \neq t_j$ for all $i \neq j$, the first term on the right-hand side of (44) is nonzero.

Now consider the vector of interarrival times $\tilde{\boldsymbol{t}} \in \mathbb{R}^6_+$, where $\tilde{t}_i = t_{i+1} w - t_i w$, $i \in \{1, 2, \ldots, 6\}$. The determinants of the matrices A and $\bar{\mathcal{O}}_{\boldsymbol{t}}$ can be written as $|A| = f_1 \sin(\tilde{t}_2) + f_2 \sin^2(\tilde{t}_2/2) + f_3 \tilde{t}_2$ and $|\bar{\mathcal{O}}_{\boldsymbol{t}}| = \tilde{f}_4 \sin(\tilde{t}_6) + \tilde{f}_6 \sin^2(\tilde{t}_6/2) + \tilde{f}_8 \tilde{t}_6$, where $\tilde{f}_i := f_i + f_{i+1} \tilde{t}_6, i \in \{4, 6, 8\}$. Note that f_1, f_2, and f_3 are continuous functions of $\tilde{t}_3$, and $\tilde{t}_4$ and f_4–f_9 are continuous functions of $\tilde{t}_1$–$\tilde{t}_5$. Furthermore, for any given $\tilde{t}_3$ and $\tilde{t}_4$, $|A|$ has countable zero crossings. Since f_1, f_2, and f_3 are continuous functions of $\tilde{t}_3$ and $\tilde{t}_4$, we can conclude that the set of points satisfying $|A| = 0$ is composed of a number of countable surfaces in $\mathbb{R}^3_+$, and is therefore a zero measure set. Using the same reasoning as for matrix A, it can be concluded that the set of points satisfying $|\bar{\mathcal{O}}_{\boldsymbol{t}}| = 0$ also has zero measure. Thus, the matrix $\mathcal{O}_{\boldsymbol{t}}$ is generically of full column rank, losing rank only at the set of zero measure sample points given by $|\bar{\mathcal{O}}_{\boldsymbol{t}}| = 0$.

Consider the particular case where the interarrival times are uniform, that is, $t_{k+1} - t_k = T$ for all $t_k \in [t_0, t_f)$. Then, it follows that $|\bar{\mathcal{O}}_{\boldsymbol{t}}(T)| = 2^{15} T^{-4} \sin^{12}(T\|\boldsymbol{\omega}_e\|/2) \sin^4(T\|\boldsymbol{\omega}_e\|)$. This implies that the matrix $\mathcal{O}_{\boldsymbol{t}}$ is of full column rank almost everywhere, losing rank only at the zero measure sample points described by the set (19). □

In Proposition 1, we showed that the matrix $\mathcal{O}_{\boldsymbol{t}}$ is full rank almost everywhere except at a set of particular sample times of zero measure defined by $|\bar{\mathcal{O}}_{\boldsymbol{t}}| = 0$. Thus, even if the matrix $\bar{\mathcal{O}}_{\boldsymbol{t}}$ is singular at a particular combination of sampling times, by slightly perturbing the sample times, it becomes nonsingular. For the nonuniform case, it is still possible to numerically conclude that for all the points in the region defined by

$$0 < t_{k+1} - t_k < \kappa \pi \|\boldsymbol{\omega}_e\|^{-1}, \quad t_k \in [t_0, t_f) \tag{45}$$

for $\kappa = 0.9$ and at least six interarrival times, $|\bar{\mathcal{O}}_{\boldsymbol{t}}| \neq 0$.

Proof (Theorem 1): Consider system (16) with the initial condition $\boldsymbol{x}_0 \in \mathbb{R}^{12}$. Let $\boldsymbol{\omega}_e \in \mathbb{R}^3$ be such that (17) holds. Without loss of generality, we consider $t_0 = 0$. The state transition matrix $\Phi(t, 0) \in \mathbb{R}^{12 \times 12}$ of (16) is given by

$$\Phi(t,0) = \begin{bmatrix} \bar{\Phi}_1(t,0) & \mathbf{0} & -t\bar{\Phi}_1(t,0) & 0 & 0 & 0 \\ \mathbf{0} & \bar{\Phi}_1(t,0) & \mathbf{0} & 0 & 0 & 0 \\ \mathbf{0} & \mathbf{0} & \bar{\Phi}_1(t,0) & 0 & 0 & 0 \\ \mathbf{0} & \mathbf{0} & \mathbf{0} & 1 & 0 & 0 \\ \mathbf{0} & \mathbf{0} & \frac{\bar{\Phi}_2(t,0)}{2} & -t & 1 & 0 \\ \bar{\Phi}_2(t,0) & \bar{\Phi}_2(t,0) & -t\bar{\Phi}_2(t,0) & t^2 & -2t & 1 \end{bmatrix} \tag{46}$$

where $\bar{\Phi}_1(t, 0)$ is the state transition matrix of the linear system $\dot{\boldsymbol{\zeta}} = -S(\boldsymbol{\omega}_e)\boldsymbol{\zeta}$ and $\bar{\Phi}_2(t, 0) = -2\int_0^t \boldsymbol{\nu}_e' \bar{\Phi}_1(s, 0) ds$. The observability matrix $\mathcal{O}_{n_r} \in \mathbb{R}^{n_r \times 12}$, $n_r \geq 7$, associated with system (16) is, according to [38], defined by

$$\mathcal{O}_{n_r} := \left[(C_{\boldsymbol{u}}(t_0)\Phi(t_0, 0))' \ \ldots \ (C_{\boldsymbol{u}}(t_{n_r - 1})\Phi(t_{n_r - 1}, 0))' \right]'$$

where $t_k \in [t_0, t_f), k \in \{0, 1, 2, \ldots, n_r - 1\}$. Note that $\mathcal{O}_{nr}$ is a function of the measurement sampling times, $t_k \in [t_0, t_f)$.

We claim that $\mathcal{O}_{n_r}$ has rank 7 almost everywhere, with the exception of a zero measure set. We show this using the rank-factorization theorem in [34, Th. 3.13]. Note that

$$\mathcal{O}_r = \begin{bmatrix} \mathbf{0} & \mathbf{0} & \mathbf{0} & 0 & 0 & 1 \\ -\boldsymbol{e}_x' & -\boldsymbol{e}_x' & \mathbf{0} & 0 & \frac{-1}{\nu_e} & 0 \\ \boldsymbol{e}_x' \times \boldsymbol{\omega}_e' & \boldsymbol{e}_x' \times \boldsymbol{\omega}_e' & \mathbf{0} & 0 & 0 & 0 \\ \boldsymbol{\omega}_e'\boldsymbol{\omega}_e\boldsymbol{e}_x' - \boldsymbol{e}_x'\boldsymbol{\omega}_e\boldsymbol{\omega}_e' & \boldsymbol{\omega}_e'\boldsymbol{\omega}_e\boldsymbol{e}_x' - \boldsymbol{e}_x'\boldsymbol{\omega}_e\boldsymbol{\omega}_e' & \mathbf{0} & 0 & 0 & 0 \\ \mathbf{0} & \mathbf{0} & 2\boldsymbol{e}_x'\boldsymbol{\omega}_e\boldsymbol{\omega}_e' & \frac{\|\boldsymbol{\omega}_e\|^2}{\nu_e} & 0 & 0 \\ \mathbf{0} & \mathbf{0} & \boldsymbol{e}_x' \times \boldsymbol{\omega}_e' & 0 & 0 & 0 \\ \mathbf{0} & \mathbf{0} & \boldsymbol{\omega}_e'\boldsymbol{\omega}_e\boldsymbol{e}_x' - \boldsymbol{e}_x'\boldsymbol{\omega}_e\boldsymbol{\omega}_e' & 0 & 0 & 0 \end{bmatrix}$$

$\mathcal{O}_{n_r} = \mathcal{O}_t(t_j, \|\boldsymbol{\omega}_e\|)\mathcal{O}_r$, $j \in \{0, 1, \ldots, n_r - 1\}$, where $\mathcal{O}_t \in \mathbb{R}^{n_r \times 7}$ whose jth row, $\mathcal{O}_{t_j}$, is given by

$$\mathcal{O}_{t_j} := 2\nu_e \begin{bmatrix} \frac{1}{2\nu_e} & t_j & \frac{1-\cos(t_j\|\boldsymbol{\omega}_e\|)}{\|\boldsymbol{\omega}_e\|^2} & \frac{t_j\|\boldsymbol{\omega}_e\| - \sin(t_j\|\boldsymbol{\omega}_e\|)}{\|\boldsymbol{\omega}_e\|^3} \\ \frac{t_j^2}{2\|\boldsymbol{\omega}_e\|^2} & t_j\frac{\cos(t_j\|\boldsymbol{\omega}_e\|) - 1}{\|\boldsymbol{\omega}_e\|^2} & \frac{t_j\sin(t_j\|\boldsymbol{\omega}_e\|)}{\|\boldsymbol{\omega}_e\|^3} \end{bmatrix}$$

and $\mathcal{O}_r \in \mathbb{R}^{7\times 12}$ is given in the equation shown at the top of this page.

Resorting to Proposition 1, it can be concluded that for almost all interarrival times, $\mathtt{Rank}(\mathcal{O}_t) = 7$. Moreover, from (17), it follows that $\mathtt{Rank}(\mathcal{O}_r) = 7$. Thus, by the rank factorization theorem, it follows that $\mathtt{Rank}(\mathcal{O}_{n_r}) = \mathtt{Rank}(\mathcal{O}_r)$.

Since $\mathtt{Rank}(\mathcal{O}_{n_r}) = \mathtt{Rank}(\mathcal{O}_r)$, we can conclude that $\mathtt{Kernel}(\mathcal{O}_{n_r}) = \mathtt{Kernel}(\mathcal{O}_r)$. Thus, the null space associated with the observability matrix is $\mathtt{Kernel}(\mathcal{O}_{n_r}) = \mathcal{N}\boldsymbol{\alpha}$, where the value of $\mathcal{N}$ is shown in (47) at the bottom of this page and $\boldsymbol{\alpha} = [\alpha_1, \ldots, \alpha_5]' \in \mathbb{R}^5$.

Note that all initial conditions of the form $\breve{\boldsymbol{x}}_0 := \boldsymbol{x}_0 + \mathcal{N}\boldsymbol{\alpha}$ are indistinguishable from $\boldsymbol{x}_0$. Since the initial condition of the beacon is known, that is, ${}^{\mathcal{B}}\breve{\boldsymbol{q}}_1(0) = {}^{\mathcal{B}}\boldsymbol{q}_1(0)$, this implies that $\alpha_1 = \omega_{e_x}\alpha_4$ and $\alpha_2 = \alpha_3 = 0$. Moreover, note that $\breve{\boldsymbol{x}}_0$ must satisfy constraints (11)–(13). Imposing constraint (12), we obtain $\alpha_5 \in \{0, -2\|\boldsymbol{\omega}_e\|^{-2}\boldsymbol{\omega}_e'(\boldsymbol{v}_e + {}^{\mathcal{B}}\boldsymbol{v}_c(0))\}$. Thus, one solution is $\alpha_5 = 0$, yielding $\alpha_4 = 0$, which is the trivial solution satisfying (11) and (13). The other nonzero solution of α_5 leads to $\alpha_4 = -2\|\boldsymbol{\omega}_e\|^{-2}\boldsymbol{\omega}_e'({}^{\mathcal{B}}\boldsymbol{p}_0(0) + {}^{\mathcal{B}}\boldsymbol{q}_1(0))$, satisfying (11) and (13), which is the set defined in (18).

To show the reverse inclusion, consider $\boldsymbol{z} := \boldsymbol{x}_0 + \boldsymbol{v} \in \mathcal{I}_r(\boldsymbol{x}_0)$, where $\boldsymbol{v} \in \mathtt{Kernel}(\mathcal{O}_r)$. Let $r(\boldsymbol{x}(t))$ denote the range output given the initial condition $\boldsymbol{x}_0$, where $\boldsymbol{x}(t)$ is the solution to (16) with $\boldsymbol{x}(0) = \boldsymbol{x}_0$ and $r(z(t))$ denotes the range output given the initial condition $\boldsymbol{z}$, where $\boldsymbol{z}(t)$ is the solution to (16) with $\boldsymbol{x}(0) = \boldsymbol{z}$. By noting that $v \in \mathtt{Kernel}(\mathcal{O}_r)$, it follows that $r(\boldsymbol{z}(t)) = C_{\boldsymbol{u}}(t)\Phi(t,0)\boldsymbol{x}_0 + C_{\boldsymbol{u}}(t)\Phi(t,0)\boldsymbol{v} = r(\boldsymbol{x}(t))$. Since $\boldsymbol{x}_0$ is an arbitrary point, by definition, system (16) combined with constraints (11)–(13) is weakly observable on $[t_0, t_f)$. The proof for the case of uniform interarrival times follows from the later part of Proposition 1. □

Note that in Theorem 1, we used the fact that $\mathtt{Rank}(\mathcal{O}_{n_r}) = \min(\mathtt{Rank}(\mathcal{O}_r), \mathtt{Rank}(\mathcal{O}_t))$. Thus, the observability condition (17) and the restriction on the interarrival times are derived independently from the matrices $\mathcal{O}_r$ and $\mathcal{O}_t$. This is because the rank of $\mathcal{O}_r$ depends only on $\boldsymbol{\omega}_e$ as $\nu_e > 0$, and the rank of $\mathcal{O}_t$ depends only on $t_k \in [t_0, t_f)$ as $\|\boldsymbol{\omega}_e\| > 0$.

Proof (Corollary 1): From Theorem 1, it follows that the set of indistinguishable points is given by (18). Suppose that there is no ocean current or ${}^{\mathcal{B}}\boldsymbol{v}_c$ in known. In this case, the set of indistinguishable points is a subset of $\{\boldsymbol{x}_0, \breve{\boldsymbol{x}}_0\}$, where $\breve{\boldsymbol{x}}_0$ is a nontrivial point in (18). Let us assume that the point $\breve{\boldsymbol{x}}_0$ is indistinguishable from $\boldsymbol{x}_0$. Since ${}^{\mathcal{B}}\breve{\boldsymbol{v}}_c = {}^{\mathcal{B}}\boldsymbol{v}_c$, we conclude that ${}^{\mathcal{B}}\boldsymbol{v}_c = {}^{\mathcal{B}}\boldsymbol{v}_c - 2\|\boldsymbol{\omega}_e\|^{-2}\boldsymbol{\omega}_e\boldsymbol{\omega}_e'({}^{\mathcal{B}}\boldsymbol{v}_c + \boldsymbol{v}_e)$, which contradicts with (20). Thus, $\breve{\boldsymbol{x}}_0$ is distinguishable from $\boldsymbol{x}_0$, and the system is observable. □

Proof (Theorem 2): Consider system (16) with the initial condition $\boldsymbol{x}_0 \in \mathbb{R}^{12}$. From (2) and (46), we conclude that $\boldsymbol{e}_z'{}^{\mathcal{I}}_{\mathcal{B}}\mathcal{R}(\boldsymbol{\eta}) = \boldsymbol{e}_z'{}^{\mathcal{I}}_{\mathcal{B}}\mathcal{R}(\boldsymbol{\eta}_e)\bar{\Phi}_1(t,0)'$.

Since $S(\boldsymbol{\omega}_e)$ is a skew symmetric matrix, it follows that $\bar{\Phi}_1(t,0)'\bar{\Phi}_1(t,0) = I, \forall t$. On the other hand, the depth measurements $\boldsymbol{y}_z$ satisfy $\boldsymbol{y}_z = C_{\boldsymbol{u},z}\Phi(t,0)\boldsymbol{x}_0 = \bar{C}_{\boldsymbol{u},z}\boldsymbol{x}_0$, where

$$\bar{C}_{\boldsymbol{u},z} = \left[\begin{bmatrix} -1 & 0 & t \\ 0 & 1 & 0 \end{bmatrix} \otimes \left(\boldsymbol{e}_z'{}^{\mathcal{I}}_{\mathcal{B}}\mathcal{R}(\boldsymbol{\eta}_e)\right) \quad \mathbf{0}\right].$$

Note that $\bar{C}_{\boldsymbol{u},z}$ is a first-order polynomial in t. Thus, each row of the observability matrix corresponding to depth-only measurements system (16) is a linear combination of rows of $\mathcal{O}_z := [I_3 \otimes (\boldsymbol{e}_z'{}^{\mathcal{I}}_{\mathcal{B}}\mathcal{R}(\boldsymbol{\eta}_e))\mathbf{0}]$.

Now, the observability of system (16) can be verified by intersecting $\mathtt{Kernel}(\mathcal{O}_r)$ derived in (47) with $\mathtt{Kernel}(\mathcal{O}_z)$. Moreover, since the initial condition of the beacon is known, from Theorem 1, it follows that $\alpha_1 = \omega_{e_x}\alpha_4$ and $\alpha_2 = \alpha_3 = 0$. Intersecting the mentioned null spaces, the following equalities must hold: $\alpha_4\boldsymbol{e}_z'{}^{\mathcal{I}}_{\mathcal{B}}\mathcal{R}(\boldsymbol{\eta}_e)\boldsymbol{\omega}_e = 0$ and $\alpha_5\boldsymbol{e}_z'{}^{\mathcal{I}}_{\mathcal{B}}\mathcal{R}(\boldsymbol{\eta}_e)\boldsymbol{\omega}_e = 0$. Now, using (15) and observing that (17) implies that $\dot{\psi}_e \neq 0$, we conclude that $\alpha_4 = \alpha_5 = 0$. Thus, the intersection of the two null spaces defined above contains only the origin, $\mathcal{I}_{rz}(\boldsymbol{x}_0) = \{\boldsymbol{x}_0\}$, and system (16) is observable on $[t_0, t_f)$. □

$$\mathcal{N} = \begin{bmatrix} \boldsymbol{e}_x & (\boldsymbol{e}_x \times \boldsymbol{\omega}_e)\omega_{e_z} & -(\boldsymbol{e}_x \times \boldsymbol{\omega}_e)\omega_{e_y} & \boldsymbol{\omega}_e - \boldsymbol{e}_x\boldsymbol{e}_x'\boldsymbol{\omega}_e & \mathbf{0} \\ -\boldsymbol{e}_x & 2\boldsymbol{\omega}_e\omega_{e_y} - (\boldsymbol{e}_x \times \boldsymbol{\omega}_e)\omega_{e_z} & 2\boldsymbol{\omega}_e\omega_{e_z} + (\boldsymbol{e}_x \times \boldsymbol{\omega}_e)\omega_{e_y} & \boldsymbol{e}_x\boldsymbol{e}_x'\boldsymbol{\omega}_e & \mathbf{0} \\ \mathbf{0} & \mathbf{0} & \mathbf{0} & \mathbf{0} & \boldsymbol{\omega}_e \\ \mathbf{0} & -2\boldsymbol{e}_y\boldsymbol{v}_e'\boldsymbol{\omega}_e\omega_{e_y} & -2\boldsymbol{e}_y\boldsymbol{v}_e'\boldsymbol{\omega}_e\omega_{e_z} & -\boldsymbol{e}_y\boldsymbol{v}_e'\boldsymbol{\omega}_e & -2\boldsymbol{\omega}_e\nu_e \end{bmatrix} \quad (47)$$

Proof (Theorem 3): Consider the system (16) with the initial condition $\boldsymbol{x}_0 \in \mathbb{R}^{12}$ and let $\boldsymbol{\omega}_e \in \mathbb{R}^3$ be such that (17) does not hold, that is, $\omega_{e_y} = \omega_{e_z} = 0$. Moreover, consider that $n_r \geq 3$ measurement samples are available.

We claim that the range-only observability matrix, $\mathcal{O}_{n_r}$, has rank 3. We show this using the rank-factorization theorem. Define $\mathcal{O}_r \in \mathbb{R}^{3\times 12}$ and $\mathcal{O}_{\boldsymbol{t}} \in \mathbb{R}^{n_r\times 3}$ whose jth row, $\mathcal{O}_{t_j}$, is given by

$$\mathcal{O}_r = \begin{bmatrix} \mathbf{0} & \mathbf{0} & \mathbf{0} & 0 & 0 & 1 \\ \boldsymbol{e}_x' & \boldsymbol{e}_x' & \mathbf{0} & 0 & \frac{1}{v_e} & 0 \\ \mathbf{0} & \mathbf{0} & 2\boldsymbol{e}_x' & \frac{1}{v_e} & 0 & 0 \end{bmatrix}$$

$$\mathcal{O}_{t_j} := v_e \begin{bmatrix} \frac{1}{v_e} & -2t_j & t_j^2 \end{bmatrix}.$$

Note that $\texttt{Rank}(\mathcal{O}_{\boldsymbol{t}}) = 3$, given $t_k - t_{k-1} > 0$. Moreover, $\texttt{Rank}(\mathcal{O}_r) = 3$. It can be verified that $\mathcal{O}_{n_r} = \mathcal{O}_{\boldsymbol{t}}(t_j)\mathcal{O}_r$, $j \in \{0, 1, \ldots, n_r - 1\}$ holds; hence, by the rank factorization theorem, it follows that $\texttt{Rank}(\mathcal{O}_{n_r}) = 3$. From a standard result in linear algebra, it follows that $\texttt{Rank}(\mathcal{O}_{n_r}) = \texttt{Rank}(\mathcal{O}_r)$. This completes the proof of the claim.

Now, using $\mathcal{O}_r$ and $\mathcal{O}_z$ from Theorem 2, it can be verified that the concatenation of the two matrices $\mathcal{O}_{rz}$ has the form

$$\mathcal{O}_{rz} = \begin{bmatrix} \begin{bmatrix} \boldsymbol{e}_y & \mathbf{0} & \mathbf{0} & \boldsymbol{e}_y & \mathbf{0} & \mathbf{0} & 2\boldsymbol{e}_z & \mathbf{0} & \mathbf{0} \end{bmatrix} & \begin{bmatrix} \frac{1}{v_e}\boldsymbol{e}_z & \frac{1}{v_e}\boldsymbol{e}_y & \boldsymbol{e}_x \end{bmatrix} \\ I_3 \otimes \left(\boldsymbol{e}_z' {}^{\mathcal{I}}_{\mathcal{B}}\mathcal{R}(\boldsymbol{\eta}_e)\right) & \mathbf{0} \end{bmatrix}.$$

In this case, the null space $\texttt{Kernel}(\mathcal{O}_{rz}) = \mathcal{N}\boldsymbol{\alpha}$, where

$$\mathcal{N} = \begin{bmatrix} \mathbf{0} & \mathbf{0} & \boldsymbol{\xi}_1 & \boldsymbol{\xi}_2 & \mathbf{0} & \mathbf{0} \\ \boldsymbol{\xi}_1 & \boldsymbol{\xi}_2 & \mathbf{0} & \mathbf{0} & \mathbf{0} & \mathbf{0} \\ \mathbf{0} & \mathbf{0} & \mathbf{0} & \mathbf{0} & \boldsymbol{\xi}_1 & \boldsymbol{\xi}_2 \\ -\boldsymbol{e}_y & \mathbf{0} & -\boldsymbol{e}_y & \mathbf{0} & -2\boldsymbol{e}_x & \mathbf{0} \end{bmatrix}$$

$\boldsymbol{\xi}_1 = \boldsymbol{e}_x + \boldsymbol{e}_z \tan\theta_e/\cos\phi_e$, $\boldsymbol{\xi}_2 = \boldsymbol{e}_y - \boldsymbol{e}_z \tan\phi_e$, and $\boldsymbol{\alpha} = [\alpha_1, \ldots, \alpha_6]' \in \mathbb{R}^6$. Imposing the constraint that the initial condition of the beacon is known yields $\alpha_1 = \alpha_2 = 0$. We thus have a fourth-order linear subspace and only three quadratic state constraints described by (11)–(13). Solving the corresponding quadratic equations, we may find a solution for α_4–α_6, but the fifth order, α_3, remains as a free parameter. This implies that the set of indistinguishable points is at least a piecewise continuous function of the free parameter α_3, and the system is not weakly observable. □

Proof (Theorem 4): The proof for the case of range-only measurements is similar to that of Theorem 1 with the only difference that we use the assumption ${}^{\mathcal{B}}\check{\boldsymbol{p}}_0(0) = {}^{\mathcal{B}}\boldsymbol{p}_0(0)$. This implies that $\alpha_1 = \alpha_4 = 0$ and $\omega_{e_z}\alpha_2 = \omega_{e_y}\alpha_3$. Moreover, note that $\check{\boldsymbol{x}}_0$ must satisfy constraints (11)–(13). Imposing constraint (12), we obtain $\alpha_5 \in \{0, -2\|\boldsymbol{\omega}_e\|^{-2}\boldsymbol{\omega}_e'({}^{\mathcal{B}}\boldsymbol{v}_c(0) + \boldsymbol{v}_e)\}$. Setting $\alpha_5 = 0$ implies $\alpha_2 = \alpha_3 = 0$, which is the trivial solution ensuring that (11) and (13) hold. The other nonzero solution of α_5 leads to

$$[\alpha_2, \alpha_3] = -[\omega_{e_y}, \omega_{e_z}]\|\boldsymbol{\omega}_e\|^{-2}\boldsymbol{\omega}_e' {}^{\mathcal{B}}\boldsymbol{p}_1(0)/\left(\omega_{e_y}^2 + \omega_{e_z}^2\right)$$

ensuring that constraints (11) and (13) hold. With two possible solutions for $\boldsymbol{\alpha}$, we conclude that $\mathcal{I}(\boldsymbol{x}_0)$ is given by (21).

Consider now the case where depth measurements are added to the set of observations (similar to the conditions in Theorem 2). The observability of system (16) can be verified by intersecting $\texttt{Kernel}(\mathcal{O}_r)$ derived in (47) with $\texttt{Kernel}(\mathcal{O}_z)$, but with the assumption that the initial condition of the AUV is known, meaning $\alpha_1 = \alpha_4 = 0$ and $\omega_{e_z}\alpha_2 = \omega_{e_y}\alpha_3$. Intersecting the mentioned null spaces, the following must hold:

$$(\omega_{e_y}\alpha_2 + \omega_{e_z}\alpha_3)\boldsymbol{e}_z' {}^{\mathcal{I}}_{\mathcal{B}}\mathcal{R}(\boldsymbol{\eta}_e)\boldsymbol{\omega}_e = 0, \quad \alpha_5 \boldsymbol{e}_z' {}^{\mathcal{I}}_{\mathcal{B}}\mathcal{R}(\boldsymbol{\eta}_e)\boldsymbol{\omega}_e = 0.$$

At this point, using (15) and noting that (17) implies that $\dot{\psi}_e \neq 0$, we conclude that $\alpha_2 = \alpha_3 = \alpha_5 = 0$. Thus, the intersection of the two null spaces defined above contains only the origin, $\mathcal{I}_{rz}(\boldsymbol{x}_0) = \{\boldsymbol{x}_0\}$, and system (16) is observable on $[t_0, t_f)$. Moreover, using the same reasoning as in Theorem 3, but with the assumption ${}^{\mathcal{B}}\check{\boldsymbol{p}}_0(0) = {}^{\mathcal{B}}\boldsymbol{p}_0(0)$, we conclude that $\mathcal{I}_{rz}(\boldsymbol{x}_0)$ is at least a piecewise continuous function of free parameter α_1. Thus, the system is not observable. □

Proof (Theorem 5): For only one beacon, the result follows from Theorems 1–4. Consider now more than one beacon. In this case, it can be concluded from (14) that the dynamic equations of each set $\{{}^{\mathcal{B}}\boldsymbol{q}_i, \chi_i, \chi_{ci}\}$ do not depend on the other sets. This means that the observability of the multiple beacon system can be investigated by analyzing the observability of each single-beacon system, and the result immediately follows from Theorems 1–4. □

ACKNOWLEDGMENT

The authors would like to thank the DSOR team—F. Almeida, J. Botelho, P. Góis, M. Ribeiro, J. Ribeiro, M. Rufino, L. Sebastião, H. Silva, and J. Soares—for their efforts in the development of the MEDUSA vehicles and their support and collaboration on the planning and execution of the sea trials.

REFERENCES

[1] J. C. Kinsey, R. M. Eustice, and L. L. Whitcomb, "A survey of underwater vehicle navigation: Recent advances and new challenges," in *Proc. IFAC Conf. Manoeuvr. Control Marine Craft*, 2006, pp. 1–12.

[2] A. P. Scherbatyuk, "The AUV positioning using ranges from one transponder LBL," in *Proc. MTS/IEEE Conf. Challenges Our Changing Global Environ. OCEANS*, vol. 3. Oct. 1995, pp. 1620–1623.

[3] M. B. Larsen, "Synthetic long baseline navigation of underwater vehicles," in *Proc. MTS/IEEE Conf. Exhibit. OCEANS*, Sep. 2000, pp. 2043–2050.

[4] T. Casey, B. Guimond, and J. Hu, "Underwater vehicle positioning based on time of arrival measurements from a single beacon," in *Proc. MTS/IEEE OCEANS*, Vancouver, BC, Canada, Sep./Oct. 2007, pp. 1–8.

[5] J. Saúde and A. P. Aguiar, "Single beacon acoustic navigation for an AUV in the presence of unknown ocean currents," in *Proc. IFAC Conf. Manoeuvr. Control Marine Craft*, 2009, pp. 298–303.

[6] S. D. McPhail and M. Pebody, "Range-only positioning of a deep-diving autonomous underwater vehicle from a surface ship," *IEEE J. Ocean. Eng.*, vol. 34, no. 4, pp. 669–677, Oct. 2009.

[7] S. E. Webster, R. M. Eustice, H. Singh, and L. L. Whitcomb, "Advances in single-beacon one-way-travel-time acoustic navigation for underwater vehicles," *Int. J. Robot. Res.*, vol. 31, no. 8, pp. 935–950, 2012.

[8] A. Bahr, J. J. Leonard, and M. F. Fallon, "Cooperative localization for autonomous underwater vehicles," *Int. J. Robot. Res.*, vol. 28, no. 6, pp. 714–728, 2009.

[9] P. Newman and J. Leonard, "Pure range-only sub-sea SLAM," in *Proc. IEEE Int. Conf. Robot. Autom.*, Sep. 2003, pp. 1921–1926.

[10] E. Olson, J. J. Leonard, and S. Teller, "Robust range-only beacon localization," *IEEE J. Ocean. Eng.*, vol. 31, no. 4, pp. 949–958, Oct. 2006.

[11] Y. Petillot *et al.*, "Acoustic-based techniques for autonomous underwater vehicle localization," *Proc. Inst. Mech. Eng. M, J. Eng. Maritime Environ.*, vol. 224, no. 4, pp. 293–307, 2010.

[12] T. L. Song, "Observability of target tracking with range-only measurements," *IEEE J. Ocean. Eng.*, vol. 24, no. 3, pp. 383–387, Jul. 1999.
[13] A. S. Gadre and D. J. Stilwell, "Underwater navigation in the presence of unknown currents based on range measurements from a single location," in *Proc. Amer. Control Conf. (ACC)*, vol. 2. Jun. 2005, pp. 656–661.
[14] A. S. Gadre, "Observability analysis in navigation systems with an underwater vehicle application," Ph.D. dissertation, Dept. Elect. Comput. Eng., Virginia Polytechnic Inst. State Univ., Blacksburg, VA, USA, 2007.
[15] P. Batista, C. Silvestre, and P. Oliveira, "Single range aided navigation and source localization: Observability and filter design," *Syst. Control Lett.*, vol. 60, no. 8, pp. 665–673, Aug. 2011.
[16] G. Indiveri and G. Parlangeli. (2013). "Further results on the observability analysis and observer design for single range localization in 3D." [Online]. Available: http://arxiv.org/abs/1308.0517
[17] F. Arrichiello, G. Antonelli, A. P. Aguiar, and A. Pascoal, "Observability metric for the relative localization of AUVs based on range and depth measurements: Theory and experiments," in *Proc. IEEE/RSJ Int. Conf. Intell. Robots Syst. (IROS)*, Sep. 2011, pp. 3166–3171.
[18] A. P. Aguiar and J. P. Hespanha, "Minimum-energy state estimation for systems with perspective outputs," *IEEE Trans. Autom. Control*, vol. 51, no. 2, pp. 226–241, Feb. 2006.
[19] R. Hermann and A. J. Krener, "Nonlinear controllability and observability," *IEEE Trans. Autom. Control*, vol. 22, no. 5, pp. 728–740, Oct. 1977.
[20] M. Bayat and A. P. Aguiar, "Underwater localization and mapping: Observability analysis and experimental results," *Ind. Robot, Int. J.*, vol. 41, no. 2, pp. 213–224, 2014.
[21] A. P. Aguiar and J. P. Hespanha, "Minimum-energy state estimation for systems with perspective outputs and state constraints," in *Proc. 42nd IEEE Conf. Decision Control*, Maui, HI, USA, Dec. 2003, pp. 4908–4913.
[22] A. J. Krener and A. Isidori, "Linearization by output injection and nonlinear observers," *Syst. Control Lett.*, vol. 3, no. 1, pp. 47–52, 1983.
[23] F. Plestan and A. Glumineau, "Linearization by generalized input-output injection," *Syst. Control Lett.*, vol. 31, no. 2, pp. 115–128, 1997.
[24] H. Nijmeijer and A. van der Schaft, *Nonlinear Dynamical Control Systems*. Berlin, Germany: Springer-Verlag, 1990.
[25] M. R. Elgersma, "Control of nonlinear systems using partial dynamic inversion," Ph.D. dissertation, Dept. Elect. Comput. Eng., Univ. Minnesota, Minneapolis, MN, USA, 1988.
[26] N. Crasta, M. Bayat, A. P. Aguiar, and A. M. Pascoal, "Observability analysis of 3D AUV trimming trajectories in the presence of ocean currents using single beacon navigation," in *Proc. 19th IFAC World Congr.*, Cape Town, South Africa, 2014, pp. 4222–4227.
[27] R. M. Murray, Z. Li, and S. S. Sastry, *A Mathematical Introduction to Robotic Manipulation*. Boca Raton, FL, USA: CRC Press, 1994.
[28] A. J. Krener, "The convergence of the minimum energy estimator," in *New Trends in Nonlinear Dynamics and Control and Their Applications* (Lecture Notes in Control and Information Science), vol. 295. Berlin, Germany: Springer-Verlag, 2003, pp. 187–208.
[29] D. Simon and T. L. Chia, "Kalman filtering with state equality constraints," *IEEE Trans. Aerosp. Electron. Syst.*, vol. 38, no. 1, pp. 128–136, Jan. 2002.
[30] S. Boyd and L. Vandenberghe, *Convex Optimization*. Cambridge, U.K.: Cambridge Univ. Press, 2004.
[31] I. Karafyllis and C. Kravaris, "From continuous-time design to sampled-data design of observers," *IEEE Trans. Autom. Control*, vol. 54, no. 9, pp. 2169–2174, Sep. 2009.
[32] V. Hassani, A. P. Aguiar, M. Athans, and A. M. Pascoal, "Multiple model adaptive estimation and model identification usign a minimum energy criterion," in *Proc. Amer. Control Conf. (ACC)*, Jun. 2009, pp. 518–523.
[33] H. K. Khalil, *Nonlinear Systems*, 3rd ed. Upper Saddle River, NJ, USA: Prentice-Hall, 2007.
[34] G. W. Stewart, *Matrix Algorithms: Basic Decompositions*, vol. 1. Philadelphia, PA, USA: SIAM, 1998.
[35] J. M. dos Santos Ribeiro, "Motion control of single and multiple autonomous marine vehicles," M.S. thesis, Dept. Elect. Comput. Eng., Inst. Superior Técnico, Lisbon, Portugal, Nov. 2011.
[36] A. J. Krener and K. Ide, "Measures of unobservability," in *Proc. 48th IEEE Conf. Decision Control (CDC)*, Dec. 2009, pp. 6401–6406.
[37] M. Bayat and A. P. Aguiar, "Observability analysis for AUV range-only localization and mapping measures of unobservability and experimental results," in *Proc. 9th IFAC Conf. Manoeuvr. Control Marine Craft*, Arenzano, Italy, 2012, pp. 325–330.
[38] J. P. Hespanha, *Linear Systems Theory*. Princeton, NJ, USA: Princeton Univ. Press, 2009.

Mohammadreza Bayat received the B.Sc. degree in electrical engineering form the Polytechnic University of Tehran, Tehran, Iran, in 2004, the M.S. degree in automation and instrumentation engineering from Petroleum University Technology, Tehran, in 2007, and the Ph.D. degree from the Instituto Superior Técnico (IST), University of Lisbon, Lisbon, Portugal, in 2015.

He is currently a Researcher with the Institute for Systems and Robotics, Instituto Superior Técnico, University of Lisbon, Portugal. His current research interests include nonlinear robust/adaptive estimation, data reconciliation, nonlinear observers, underwater robot localization, and tracking.

Naveena Crasta received the B.E. degree in electrical and electronics engineering from the Manipal Institute of Technology, Manipal, India, in 2000, the M.Tech. degree in control and automation from IIT Delhi, Delhi, India, in 2004, and the Ph.D. degree in aerospace engineering from IIT Bombay, Mumbai, India, in 2009.

He is currently a Researcher with the Institute for Systems and Robotics, Instituto Superior Técnico, University of Lisbon, Lisbon, Portugal. His current research interests include nonlinear systems theory, dynamics and control of rotational motion, control, navigation, and guidance of autonomous robotic vehicles, nonlinear observers and estimation theory, energy-based control and computational geometry.

António Pedro Aguiar (M'02) received the Licenciatura, M.S., and Ph.D. degrees in electrical and computer engineering from the Instituto Superior Técnico (IST), University of Lisbon, Lisbon, Portugal, in 1994, 1998, and 2002, respectively.

He was a Post-Doctoral Researcher with the Center for Control, Dynamical-Systems, and Computation, University of California at Santa Barbara, Santa Barbara, CA, USA, from 2002 to 2005. From 2005 to 2012, he was a Senior Researcher with the Institute for Systems and Robotics/IST, and an invited Assistant Professor with the Department of Electrical and Computer Engineering, IST. He is currently an Associate Professor with the Department of Electrical and Computer Engineering, Faculty of Engineering, University of Porto, Porto, Portugal. His current research interests include modeling, control, navigation, and guidance of autonomous robotic vehicles, nonlinear control, switched and hybrid systems, tracking, path-following, performance limitations, nonlinear observers, the integration of machine vision with feedback control, networked control, and coordinated/cooperative control of multiple autonomous robotic vehicles.

António M. Pascoal (M'82) received the Ph.D. degree in control science from the University of Minnesota, Minneapolis, MN, USA, in 1987.

He was an Instituto Superior Técnico's (IST) Responsible Scientist for eight EU funded collaborative research projects and several national research projects, all in the area of dynamical systems and ocean/air robotics. He has cooperated extensively with groups in Europe, USA, India, and Korea on the development and sea testing of robotic systems for ocean exploration. He is currently an Associate Professor of Control and Robotics with IST, University of Lisbon, Lisbon, Portugal. He is a member of the Scientific Council of the Institute for Systems and Robotics, Lisbon. His expertise is dynamical systems theory, robotics, navigation, guidance, and control of autonomous vehicles, and networked control and estimation. His long-term goal is to contribute to the development of advanced technological systems for ocean exploration and exploitation aimed at bridging the gap between science and technology.

Dr. Pascoal was the Elected Chair of the IFAC Technical Committee Marine Systems from 2008 to 2014.